February 5, 1988

Annual Report for Grant No. NAGW-319 Basic
Covering the Period from 15 January 1987 to 15 January 1988

PHOTOABSORPTION AND PHOTODISSOCIATION OF MOLECULES IMPORTANT IN THE INTERSTELLAR MEDIUM

Submitted by:

Long C. Lee and Masako Suto
Department of Electrical & Computer Engineering
San Diego State University
San Diego, CA 92182

Prepared for:

NASA Headquarters
Washington, D.C. 20546
Attention: Dr. Fred Gillett
Astronomy/Relativity Branch
Code EZ

TABLE OF CONTENTS

I. INTRODUCTION

This report describes the research results obtained in the period from January 15, 1987 to January 15, 1988 for the research program supported by NASA under Grant No. NAGW-319. The Photo-absorption and photodissociation cross sections of interstellar molecules and radicals were measured in the 90-200 nm region using synchrotron radiation, F_2 laser, excimer lasers, and discharge lamps as light sources. These data are currently needed for determining the formation and destruction rates of molecules and radicals by the interstellar radiation field.

II. RESEARCH ACCOMPLISHED

The research results accomplished in the period from January 15, 1987 to January 15, 1988 are summarized below:

A. Photoabsorption and Photodeposition of H_2S and D_2S

H_2S is quite abundant in the interstellar medium. The photoabsorption and photodissociation cross sections of H_2S and D_2S were measured, and the results were published in the Journal of Chemical Physics. A reprint of the paper is attached as Appendix A.

B. Photoabsorption and Photodissociation of CH_3Cl, CH_2Cl_2, $CHCl$, and CCl_4

photodissociation of chloromethanes (CH_nCl_{4-n}; n=1-3) may produce CH_n radicals that are important in the study of interstellar photochemistry. The photodissociation cross sections of these molecules are the most fundamental information needed to determine the concentrations of the CH_n radicals; and

these data were measured in this research program. All the studied molecules show broad absorption bands, indicating that photoabsorption of these molecules lead to dissociation. The photoabsorption cross section is thus essentially equal to the photodissociation cross section. The results are described in more detail in a paper attached as Appendix B.

C. Photoabsorption and Photodissociation of HCOOH, $HCOOCH_3$, and CH_3COOH

Formic acid (HCOOH) and acetic acid (CH_3COOH) are abundant in the interstellar medium. Their photoabsorption and photodissociation cross sections are needed to determine their lifetimes in the interstellar clouds, and they were measured in the 105-250 nm region. Emissions from excited HCOO photofragment were observed from photoexcitation of HCOOH and $HCOOCH_3$, and their fluorescence cross sections were measured. The results are summarized in a paper attached as Appendix C.

D. Photoexcitation of CH_3

CH_3 is an important interstellar radical. The Photoexcitation process of CH_3 is of interest for the study of the hydrocarbon cycle in the interstellar photochemistry. CH_3 was produced by either photodissociation of CH_3Cl or by reactions of CH_4 with F and Cl atoms, which were produced by a microwave discharge of trace F_2 and Cl_2 in He. The CH(A, B --> X) emissions were observed when CH_3 was excited by F_2 laser photons (157.5 nm) by a single-photon process and by ArF laser photons (193 nm) by a two-photon process. This emission is a useful means for the detection of CH_3. We will use the current result as a base for

the measurement of CH_3 photoabsorption cross section. The result for the study of CH_3 is summarized in a paper attached as Appendix D.

E. Photoabsorption of ^{13}CO

CO is one of the most abundant interstellar molecules. The photoabsorption cross sections of both ^{12}CO and ^{13}CO are needed for understanding the photochemistry of interstellar clouds. The photoabsorption cross section of ^{12}CO has been measured, but the cross section for the absorption continua are still not certain. We will continue the measurement in the next funding period.

The photoabsorption cross section of ^{13}CO has been measured in the current funding period. The preliminary result shows that the photoabsorption spectrum of ^{13}CO is slightly different from that of ^{12}CO. The photoabsorption cross sections of ^{13}CO and ^{12}CO will be analyzed in the next funding period.

III. Publications and Presentations in this Reporting Period

1. L. C. Lee, X. Wang, and M. Suto, "Quantitative Photoabsorption and Fluorescence Spectroscopy of H_2S and D_2S at 49-240 nm," J. Chem. Phys., 86, 4353 (1987).

2. L. C. Lee and M. Suto, "Fluorescence Yields from Photodissociative Excitation of Chloromethanes by Vacuum Ultraviolet Radiation," Chem. Phys. 114, 423 (1987).

3. M. Suto, C. Ye, C. T. Cheah, and L. C. Lee, "Emissions from Photodissociative Excitation of CH_3 Radicals," presented at the 1987 Pacific Conference on Chemistry and Spectroscopy, Orange County, Calif., Oct. 28-30, 1987.

4. M. Suto, X. Wang, and L. C. Lee, "Fluorescence Yields from Photodissociative Excitation of HCOOH, $HCOOCH_3$, and CH_3COOH in Vacuum Ultraviolet," submitted to J. Phys. Chem. (1987).

5. C. Ye, M. Suto, and L. C. Lee, "CH(A-X, B-X) Emissions from Photodissociative Excitation of CH_3," Submitted to J. Chem. Phys. (1987).

Appendix C

Fluorescence Yield from Photodissociative Excitation of $HCOOH$, $HCOOCH_3$, and CH_3COOH in Vacuum Ultraviolet

Fluorescence Yields from Photodissociative Excitation of $HCOOH$, $HCOOCH_3$ and CH_3COOH in the Vacuum Ultraviolet

Masako Suto*, Xiuyan Wang, and L. C. Lee[a)]
Department of Electrical & Computer Engineering
San Diego State University
San Diego, California 92182

ABSTRACT

The photoexcitation processes of $HCOOH$, $HCOOCH_3$ and CH_3COOH were studied in the vacuum ultraviolet region using synchrotron radiation and a pulsed discharge lamp as light sources. The absorption and fluorescence cross sections of these molecules were measured in the 106-260 nm region. Fluorescences were detected from photoexcitation of $HCOOH$ and $HCOOCH_3$, but not from CH_3COOH. Fluorescence produced at 123.9 nm was dispersed and identified as the excited OH and HCOO radicals. Fluorescence quantum yields of $HCOOH$ and $HCOOCH_3$ increase with decreasing excitation wavelengths with maxima of 5% and 0.3% at 106 nm, respectively.

a) Also, Department of Chemistry, San Diego State University

I. Introduction

Fluorescences from photodissociative excitation of HCOOX (X=H, Me, and Et) were observed a long time ago by Style and Ward.[1] The emitter was attributed to the excited HCOO radical.[1-3] However, the HCO_2 emission was not shown in the fluorescence spectrum reported by Vinogradov and Vilesov,[4] when HCOOH was excited by vacuum ultraviolet (VUV) radiation. They attributed the fluorescence to the OH(A-X) system, but not to HCOO. It is of interest to elucidate this difference.

The photoabsorption of HCOOH has been extensively investigated both in the VUV and UV regions.[4-15] The Rydberg series shown in the absorption spectrum were well assigned, but the valence states were not identified.[13] The photoabsorption of $HCOOCH_3$ is less extensively studied[5,9,10] than that of HCOOH. The absorption spectra of carboxyl compounds show similarity, because the absorption is mainly induced by the active electrons in the common C=O bond.

The photodissociative excitation processes of carboxyl compounds are little studied. To the authors' knowledge, the fluorescence yield of HCOOH given by Vinogradov and Vilesov[4] is the only study related to this subject. However, their absorption spectrum is quite different from the published data[5] and their fluorescence spectra are not consistent with other observations.[1] Thus, the cross sections for the production of fluorescence from photodissociative excitation of HCOOH and $HCOOCH_3$ are essentially not known; and these data are reported in

this paper. In order to confirm the emitting species, the photoexcitation process of CH_3COOH was also studied, and the result is included in this paper. The fluorescence yield of this molecule is too small to observe. This result is again different from the observation of Vinogradov and Vilesov[4] who reported a substantial fluorescence yield.

In addition to fundamental interest in understanding photoexcitation processes, the current results are useful for the study of photochemistry in the Earth's upper atmosphere and the interstellar medium. Formic and acetic acids are detected in the upper troposphere and in rainwater.[16-19] The formation and destruction mechanisms of these organic acids both in the gas and liquid phases are needed for understanding their roles in the formation process of acid rain.[20,21] HCOOH and $HCOOCH_3$ have been detected in the interstellar diffuse clouds.[22-25] Their photodissociation cross sections are needed for calculation of their photodissociation rates in the interstellar radiation field.[26]

II. EXPERIMENTAL

The experimental set-up for the synchrotron radiation measurement has been described in a previous paper.[27] In brief, synchrotron radiation produced from the 1-GeV electron storage ring at the University of Wisconsin was dispersed by a 1-m vacuum monochromator. The optical path length was 41.1 cm. Absorption cross sections were measured according to Beer's law. The linear dependence of absorbance on pressure was observed, and the

photoabsorption cross section was determined from the slope. It is noted that the measured absorption cross sections of a sharp band depends on the monochromator slit width. The UV-visible fluorescence was monitored by a cooled PMT (EMI 9558QB) sensitive in the 180-800 nm region. The fluorescence was simultaneously observed with the photoabsorption measurement in a direction perpendicular to the incident photon beam.

For the fluorescence dispersion experiment, the sample gas was irradiated by a Ny line at 123.9 nm produced from a capillary-condensed-discharge light source which was isolated by a 1-m vacuum monochromator (McPherson 225). The fluorescence was dispersed by a 0.3-m monochromator (McPherson 218) and detected by a cooled PMT (EMI 9558QB). Signal from the PMT was processed by a gated photon counter (EG&G ORTEC)

Samples of HCOOH (96.8% purity) and $HCOOCH_3$ (99.8%) were obtained from Sigma Chemical Co. CH_3COOH was supplied by Fisher with a purity of 99.7%. The sample gases were degassed at 97 K prior to use for measurements. The major impurity in HCOOH was water. The gas cell was continuously pumped by a sorption pump to maintain a constant pressure. This flow system minimized the contamination by impurities produced from photodissociation of sample gas and outgassing of walls. The pressure in the gas cell was monitored by a MKS Baratron manometer.

Both HCOOH and CH_3COOH form dimers in the gas phase. The concentration ratio of dimer to monomer is negligibly small at pressures lower than 50 mtorr.[28,29] If high vapor pressure was

used, a small fraction of absorption is due to dimers. The measurements were done at room temperature (22 ^{o}C).

III. RESULTS AND DISCUSSION

A. Fluorescence Spectra

The fluorescence spectra from photoexcitation of HCOOH and $HCOOCH_3$ at 123.9 nm are shown in Fig. 1(a) and 1(b), respectively. Both spectra, which consist of the OH(A-X) band at 310 nm and a broad continuum in the 330-500 nm region, are similar. The emission spectrum from photoexcitation of CH_3COOH at 123.9 nm was also examed as shown in Fig. 1(c). The emission signal from this molecule does not differ from the background shown in Fig. 1(d), which was taken with no gas in the gas cell. This result indicates that the emission from CH_3COOH is not detectable.

When one atmosphere of He was added to the gas cell, vibrational bands of the emission from HCOOH and $HCOOCH_3$ photolysis appear in the fluorescence spectra as shown in Fig. 2. This is due to rotational and vibrational relaxation of the excited state(s) to low vibrational level(s) by collision with added helium. The vibrational structure is related to the vibrational progression(s) of the lower state. The vibrational bands are classified into two vibrational progressions with an average frequency spacing of 1195 cm^{-1}. These progressions are shifted to each other by about 690 cm^{-1}. It is noted that the OH emission bands also become sharper when He is added.

Style and Ward[1] have observed emissions from photoexcitation of HCOOH, DCOOH, DCOOD, HCOOMe and HCOOEt. The emission spectra are similar when hydrogen atoms were replaced by deuterium. The fluorescence spectra from methyl and ethyl formates were very similar to that of HCOOH except for broadening. Thus, they concluded that the emitting species responsible for this blue fluorescence in the 330-500 nm region is the HCOO radical. Later, Peacock et al.[3] reexamined this emission system by molecular orbital calculation and concluded that the fluorescence is indeed due to HCOO. The blue emission was also observed from the collisions of HCOOH with metastable Ar ($^3P_{2,0}$) atom.[30] The current results further confirm that the emitting species is the HCOO radical, but not COOH.

For the HCOOH photolysis, the OH fluorescence intensity is only about 8% of the HCOO emission as shown in Fig. 1(a). This is quite different from the result of Vinogradov and Vilesov who did not report the HCOO emission.[4] The OH emission may partly originate from the photolysis of H_2O which may exist as impurities. However, the H_2O contribution may not be significant, because the H_2O spectra do not appear in the absorption and fluorescence excitation spectra of HCOOH as discussed in the next section.

The fluorescence spectrum from the photolysis of $HCOOCH_3$ in the 300-350 nm region (see Fig. 1(b)) is mainly due to the OH(A-X) emission. It may possibly contain the $CH_3O(\tilde{A}-\tilde{X})$ system[31]. The CH_3O emission may be produced from photolysis of $HCOOCH_3$.

However, it is not certain whether the CH_3O emission is present, because characteristic vibrational strucure of the CH_3O emission[31] is not clear in Fig.1(b). The OH emission is likely from the H_2O impurities. Since the fluorescence cross section of $HCOOCH_3$ is relatively small (as discussed in the next section), the OH emission shows up more distinctly in Figs. 1(b) and 2(b).

B. Photoabsorption and Fluorescence Cross Sections

B.1 HCOOH

The absorption cross section of HCOOH was measured in the 106-250 nm region as shown in Figs. 3(a) an (b). In the 106-180 nm region, the absorption cross sections were measured at low gas pressure so that the data were free from the interference of dimers. The experimental uncertainties are estimated to be + 10% of the given values. Present values agree well with those measured by Barnes and Simpson,[5] except that the current peak cross sections are generally higher than theirs because of high monochromator resolution in the current work. The data of Nagakura et al.[9] are higher than the current ones.

Since the absorption cross section in the 180-250 nm region is very small, relatively high pressures (up to 1 torr) were used for the measurement. HCOOH tends to form dimers at high pressure. For example, in 1 torr of HCOOH vapor, about 30% of the molecules are dimers.[28,29] The absorption cross sections of HCOOH monomer and dimer have been extensively studied by

Singleton et al.[15] The dimer effect is not corrected for the absorption spectrum shown in Fig. 3(b).

The excited states of HCOOH have been studied by the photographic absorption spectra[8,10] and the electron-energy-loss spectrum.[11,12] Three Rydberg series converging to the ionization limit at 109.41 nm (11.332 eV)[32-34] were classified with quantum defects of 0.85, 0.6 and 0.14 for the transitions of s, p and d Rydberg orbitals, respectively.[8,10] The early members of each series have vibrational progressions with a vibrational frequency of about 1500 cm^{-1}. The vibrational frequency and the intensity pattern are very similar to the photoelectron spectrum of the ground state of the HCOOH ion.[35,36]

The ground state of the ion is planar and the vibrational frequency of C=O stretching (ν_3 mode) is about 1500 cm^{-1}, while the ground state of neutral HCOOH is non planar and the ν_3 vibrational frequency is 1770 cm^{-1}. The Rydberg states assigned by Bell et al.[10] and the excited states classified by Herzberg[37] are indicated in Fig. 3. Fridh[11] has reclassified the Rydberg states into three p type Rydberg series (npa'σ, npa'π and npa"). The npa'σ and npa'π series correspond to the ns and np series of Bell et al.[10], respectively. The first mumber of npa" series exists in the $\tilde{C}$ state. The nd series of Bell et al.[10] is assigned to the nsa' series with δ=1.14, in which the first member at the $\tilde{D}$ state is the 4sa' state.

The presence of valence states in the region of the $\tilde{C}$ and $\tilde{B}$ states has been discussed by Robin.[13] The $n_O \longrightarrow \sigma^*$ valence

transition may exist around 138 nm ($\tilde{C}$ state).[13] The $\tilde{B}$ state has been assigned to the $n_O \longrightarrow 3s$ Rydberg transition by Bell et al.[10], but it was assigned to the $\pi_2 \longrightarrow \pi^*$ valence transition by Barnes and Simpson.[5] The broad continuum in the 160-185 nm region has been assigned to the $\pi_2 \longrightarrow \pi^*$ valence transition by Bell et al.[10] and Nagakura et al.[9], but it was assigned to the 3sa' Rydberg state by Fridh.[11] The $\tilde{A}$ state in the UV region is assigned to the $n_O \longrightarrow \pi^*$ valence transition. The long vibrational progression in the 225-260 nm region has a frequency of 1080 cm^{-1} (ν_3, C=O stretching mode) associated with sub-bands of 400 cm^{-1} (ν_7, OCO bending mode), which has been investigated by Ng and Bell.[7]

Fluorescence was observed from the photolysis of HCOOH at excitation wavelengths shorter than 140 nm. Emissions are due to HCOO and OH radicals as discussed above. At low gas pressure, the fluorescence intensity is given by,

$$I_f = CF\sigma_f In \qquad (1)$$

where C is the geometrical constant, F is the detection efficiency of the PMT, σ_f is the fluorescence cross section, I is the intensity of dispersed synchrotron radiation , and n is the concentration of the sample gas. Equation (1) is valid only when the loss of the excited fragments due to quenching can be neglected. The detection efficiency of the PMT is considered to be same for both emissions of OH at 310 nm and HCOO at 350-500 nm. Thus, CF in Equation (1) can be evaluated by measureing the OH emission intensity from the photolysis of H_2O, of which

fluorescence cross section is known.[27] The fluorescence intensity from HCOOH photolysis was converted to the absolute fluorescence cross section. The cross section for the production of fluorescence in the 200-800 nm region is shown in Fig. 3(a). The experimental uncertainty is about 30% of the given values. The fluorescence cross section in the 130-140 nm region is very small. The fluorescence excitation spectrum generally follows the absorption spectrum, except for a small difference in the 120-130 nm region.

In the fluorescence cross section measurements, optical filters were used to isolate the HCOO emission from the OH band. The fraction of the OH emission in the total fluorescence cross section shown in Fig.3(a) is estimated to be less than 10%. This result is consistent with the fluorescence dispersion experiment that the HCOO emission is dominant. The contamination from water impurity is very small, because the characteristic bands of H_2O do not show up in both the absorption and fluorescence excitation spectra of Fig. 3(a).

B. 2 $HCOOCH_3$

The absorption cross section of $HCOOCH_3$ was measured in the 106-250 nm region as shown in Figs. 4(a) and 4(b). The current measurement agrees with the data of Barnes and Simpson in the 124-250 nm region.[5] The absorption spectrum shows band structure superimposing on continua. The absorption spectrum of $HCOOCH_3$ is similar to that of HCOOH. By analogy with HCOOH, the excited states of $HCOOCH_3$ are labelled as shown in Fig. 4. The $\tilde{A}$ state

is probably the $n_o \longrightarrow \pi^*$ valence transition with a weak vibrational band of frequency about 980 cm^{-1}. The absorption bands are likely the Rydberg states converging to the first ionization potential at 10.815 eV (114.64 nm).[33] Some of the prominent peaks in the $\tilde{C}$ and $\tilde{D}$ states are separated by about 1400 cm^{-1}, which is likely the C=O stretching vibration as observed in HCOOH and CH_3COOH. In the $\tilde{E}$ and $\tilde{F}$ states, there are a number of weak vibrational subbands with frequencies of 200~400 cm^{-1},

Fluorescence from photoexcitation of $HCOOCH_3$ appears at excitation wavelengths shorter than 134 nm. The fluorescence cross section is shown in Fig. 4(a). The fluorescence excitation spectrum follows the absorption spectrum, except for fine structure that is not apparent in the fluorescence excitation spectrum. The fluorescence cross section of $HCOOCH_3$ is about one order of magnitude smaller than that of HCOOH, in contrast to the absorption cross section being the same order of magnitude. The contamination by water impurity is small, because the characteristic bands of H_2O do not appear in both absorption and fluorescence excitation spectra.

B. 3 CH_3COOH

In order to conform the emitting species from HCOOH and $HCOOCH_3$, the photoabsorption and fluorescence cross sections of CH_3COOH were also investigated in this experiment. The absorption cross section in the region of 106-240 nm is shown in Fig. 5. The absorption spectral envelope agrees generally with those of Bell et al.[10] and Barnes and Simpson.[5] However, the

current absolute values are generally lower than those measured by Barnes and Simpson in the 125-250 nm region[5] and Nagakura et al.[9] in the 155-190 nm region. The absorption cross sections at wavelengths longer than 190 nm are small; thus, high gas pressures (up to 0.7 torr) were used for the measurement. The dimers may contribute to the measured absorption cross section, for which the correction is not applied.

Absorption of CH_3COOH consists of several broad bands superimposing on continua. The excited states were labelled as $\tilde{A}$, $\tilde{A}'$, $\tilde{B}$, $\tilde{C}$, etc., by Bell et al.[10], in analogy with HCOOH. The $\tilde{A}'$ state was not observed by Nagakura et al.[9] The excited states at wavelengths shorter than 155 nm are likely the Rydberg series converging to the first ionization potentials at 10.35 eV[32] or 10.644 eV.[34] Vibrational structures appear in the $\tilde{C}$, $\tilde{D}$, and $\tilde{E}$ states. The vibrational frequency is about 1450 cm^{-1}, which corresponds to the C=O stretching frequency.[10]

No detectable fluorescence was observed from photoexcitation of CH_3COOH in the entire wavelength region studied. The fluorescence cross section of CH_3COOH is smaller than a detection limit of 5×10^{-21} cm^2. The result of the synchrotron radiation experiment is consistent with the fluorescence dispersion experiment shown in Fig.1(c) that the fluorescence signal is not detectable.

C. Fluorescence Yields

The fluorescence quantum yield is defined as a ratio of fluorescence cross section to absorption cross section. The

fluorescence yield of HCOOH is shown in Fig. 6. The yield increases with decreasing wavelength with a value of about 5% at 106 nm. This trend is consistent with the result of Vinogradov and Vilesov,[4] although they attributed of the emission to the OH system in contrast to the current study.

The quantum yield of fluorescence from the photolysis of $HCOOCH_3$ is shown in Fig. 7. The fluorescence yield starts to appear around 134 nm and increases with decreasing excitation wavelength. The maximum yield is about 0.3% at 106 nm, which is much smaller than that of HCOOH. This small yield may be caused by the fact that $HCOOCH_3$ has higher degree of freedom than HCOOH such that the probability for dissociation into the emission channel is small. Similar trends are observed in many cases, for example, HCN[38] versus CH_3CN[39] and H_2O[27] versus CH_3OH.[40]

The quantum yields of emission from HCOOH and $HCOOCH_3$ photolysis are essentially a smooth function of the excitation wavelength, except for HCOOH in the 125-135 nm region, where structure is observed. The fluorescence yield is a measure of the interaction strength between the initial excited state and the dissociative states that produce the emitting species. The smooth function of the quantum yield indicates that the interaction strength is the same regardless the initial excited state is a continuum or a discrete state.

The upper limit for the fluorescence yield from CH_3COOH is estimated to be 0.02%. This value is much smaller than the data of Vinogradov and Vilesov[4], who reported a significant

fluorescence yield at wavelengths shorter than 125 nm. Their value at 106 nm is 0.2%.

D. Photodissociation Processes

The possible dissociative processes of HCOOH that produce the emitting species are;

$$HCOOH \longrightarrow HCO + OH \quad (2)$$

$$\longrightarrow HCOO + H \quad (3)$$

The enthalpy changes in processes (2) and (3) are 110.2 and 166.6 kcal/mol, respectively.[41,42] The threshold wavelength to produce OH*(A) by process (2) is 140.4 nm. Vinogradov and Vilesov[4] determined the threshold to be at (141 ± 1) nm. However, the current result of Fig. 3(a) does not show significant fluorescence cross section at wavelengths longer than 135 nm. The potential energy of the excited state of HCOO is not known. Since HCOO emits at wavelengths longer than OH, the threshold wavelength for producing the HCOO emission must be longer than 140 nm. The observed fluorescence threshold at 135 nm is shorter than the expected value.

The possible dissociative processes of $HCOOCH_3$ that produce the emitting species are,

$$HCOOCH_3 \longrightarrow HCO + CH_3O \quad (4)$$

$$\longrightarrow HCOO + CH_3 \quad (5)$$

The enthalpy changes in (4) and (5) are 97.5 and 82.42 kcal/mol, respectively.[41,42] The threshold to produce the HCOO emission via process (5) is estimated at about 174 nm assuming that the (0-0) transition of the HCOO emission is around 350 nm. The

observed threshold at 134 nm is much shorter than estimated. The fluorescence intensity at the calculated threshold is too weak to be detectable; this may be caused by the unfavorable Franck-Condon factor for the production of the emitting species at the threshold and/or by a potential barrier between the initial excited state and the dissociative channel that produces the emitting species.

The photodissociation processes of HCOOH in the UV region have been studied recently. The quantum yield of process (2) is about 1 at 222 nm.[43] It is likely that process (2) is also a major channel in the VUV region, although no quantitative data are available. Other channels such as HCOO+H, H_2+CO_2, etc., are possible at high excitation energy. Since the fluorescence yields are so small, the photoexcitation of HCOOH in the VUV region may mostly produce fragments in the electronic ground states. In that case, large excess energy may be dissipated as kinetic, rotational and vibrational energies of fragments.

CONCLUDING REMARKS

Photoabsorption and fluorescence cross sections of HCOOH, $HCOOCH_3$, and CH_3COOH were measured in the 106-260 nm region using synchrotron radiation as a light source. The fluorescence spectra were dispersed and identified as the OH(A-X) and HCOO systems. The fluorescences were observed from HCOOH and $HCOOCH_3$ at excitation wavelengths shorter than 140 and 134 nm, respectively. The fluorescence yields increase with decreasing

wavelengths with maximum yields of 5% for HCOOH and 0.3% for $HCOOCH_3$ at 106 nm. No emissions was detected from VUV photolysis of CH_3COOH.

ACKNOWLEDGEMENT

The authors are grateful to the staff of the Synchrotron Radiation Center (SRC) at the University of Wisconsin for providing the VUV light source. The SRC facility is supported by the NSF. This material is based on the work supported by the NSF and the NASA.

REFERENCES

1. Style, D. W. G.; Ward, J. C., J. Chem. Soc. 1952, 2125.
2. Style, D. W. G.; Ward, J. C., Trans. Faraday Soc. 1953, 49, 999.
3. Peacock, T. E.; Rahman, R. -U.; Sleeman, D. H.; Tuckley, E. S. G., Disc. Faraday Soc. 1963, 35, 144.
4. Vinogradov, I. P.; Vilesov, F. I., Khim. Vys. Energ. 1977, 11, 25.
5. Barnes, E. E.; Simpson, W. T., J. Chem. Phys. 1963, 39, 670.
6. Sugarman, B., Proc. Phys. Soc., 1943, 55, 429.
7. Ng, T. L.; Bell, S., J. Mol. Spectrosc. 1974, 50, 166.
8. Price, W. C.; Evans, W. M., Proc. R. Soc. London, 1937, A 162, 110.
9. Nagakura, S.; Kaya, K.; Tsubomura, H., J. Mol. Spectrosc. 1964, 13, 1.
10. Bell, S.; Ng, T. L.; Walsh, A. D., J. Chem. Soc. Faraday 2, 1975, 71, 393.
11. Fridh, C., J. Chem. Soc. Faraday 2, 1978, 74, 190.
12. Ari, T; Hasted, J. B., Chem. Phys. Lett. 1982, 85, 153.
13. Robin, M. B., "Higher Excited States of Polyatomic Molecules," Vol. 3, Academic, New York, 1985.
14. Wine, P. H.; Astalos, R. J.; Mauldin III, R. L., J. Phys. Chem. 1985, 89, 2620.
15. Singleton, D. L.; Paraskevopoulos, G.; Irwin, R. S. J. Photochem., 1987, 37, 209.

16. Dawson, G. A.; Farmer, J. C.; Moyers, J. L., Geophys. Res. Lett. 1980, 7, 725.

17. Goldman, A.; Murcray, F. H.; Murcray, D. G.; Rinsland, C. P., Geophys. Res. Lett., 1984, 11, 307.

18. Galloway, J. N.; Linkins, G. E.; Keene, W. C.; Miller, J. M., J. Geophys. Res. 1982, 87, 8771.

19. Keene, W. C. and Galloway, J. N., J. Geophys. Res. 1986, 91, 14,466.

20. Chameides, W. L.; Davis, D. D., Nature, 1983, 304, 427.

21. Chameides, W. L., J. Geophys. Res. 1984, 89, 4739.

22. Churchwell, E.; Nash, A.; Rahe, J.; Walmsley, C. M.; Lochner, O.; Winnewisser, G., Astrophys. J. 1980, 241, L169.

23. Ellder, J.; Friberg, P.; Hjalmarson, A.; Hoglund, B.; Irvine, W. M.; Johansson, L. E. B.; Olofsson, H.; Rydbeck, G.; Rydbeck, O. E. H.; Guelin, M., Astrophys. J. 1980, 242, L93.

24. Dalgarno, A.; Black, J. H., Rep. Prog. Phys., 1976, 39, 573.

25. Watson, W. D., Rev. Mod. Phys. 1976, 48, 513.

26. Lee, L. C., Astrophys. J. 1984, 282, 172.

27. (a) Lee, L. C., J. Chem. Phys. 1980, 72, 4334 : (b) Lee, L.C.; Suto, M., Chem. Phys. 1986, 110, 161

28. Halford, J. O., J. Chem. Phys. 1942, 10, 582.

29. Barton, J. R.; Hsu, C. C., J. Chem. Eng. Data 1969, 14, 184.

30. Clyne, M. A. A.; Coxon, J. A.; Setser, D. W.; Stedman, D. H., Trans. Faraday Soc. 1969, 65, 1177.

31. Wantuck, P. J.; Oldenborg, R. C.; Baughcum, S. L.; Winn, K. R., J. Phys. Chem. 1987, 91, 3253.

32. Watanabe, K., J. Chem. Phys. 1957, 26, 542.

33. Watanabe, K.; Nakayama, T.; Mottl, J., J. Quant. Spectrosc. Radiat. Transfer. 1962, 2, 369.

34. Knowles, D. J.; Nicholson, A. J. C., J. Chem. Phys. 1974, 60, 1180.

35. Brundle, C. R.; Turner, D. W.; Robin, M. B.; Basch, H., Chem. Phys. Lett. 1969, 3, 292.

36. Watanabe, I.; Yokoyama, Y.; Ikeda, S., Chem. Phys. Lett. 1973, 19, 406.

37. Herzberg, G., "Electronic Spectra and Electronic Structure of Polyatomic Molecules," Van Nostrand Reihold, New York 1966.

38. Lee, L. C., J. Chem. Phys. 1980, 72, 6414.

39. Suto, M.; Lee, L. C., J. Geophys. Res. 1985, 90, 13037.

40. Nee, J. B.; Suto, M.; Lee, L. C., Chem. Phys. 1985, 98, 147.

41. Benson, S. W. "Thermochemical Kinetics," Wiley, New York 1976.

42. Chase Jr., M. W.; Davies, C. A.; Downey Jr., J. R.; Frurip, D. J.; McDonald, R. A.; Syverud, A. N., "JANAF Thermochemical Table," 3rd ed., J. Phys. Chem. Reference Data, 1985, 14, Suppl. 1.

43. Jolly, G. S.; Singleton, D. L.; Paraskevopoulos, G., J. Phys. Chem. 1987, 91, 3463.

FIGURE CAPTIONS

Fig. 1. Fluorescence spectra excited by Ny 123.9 nm. (a) HCOOH, (b) $HCOOCH_3$, (c) CH_3COOH and (d) background. The detection response is shown in (a) as the dashed line.

Fig. 2. Fluorescence spectra from (a) HCOOH and (b) $HCOOCH_3$ in presence of 1 atmosphere of He.

Fig. 3. Absorption (——) and fluorescence (---) cross sections of HCOOH. The cross section is in units of Mb (10^{-18} cm^2/molec.). Assignment of excited states are indicated based on the assignment by Bell et al. The absorption cross section in the 180-250 nm region is affected by dimer (see text).

Fig. 4. The absorption (——) and fluorescence (---) cross sections of $HCOOCH_3$ in the 106-250 nm region. The cross section is in units of Mb (10^{-18} cm^2/molec.).

Fig. 5. The absorption cross section of CH_3COOH. The cross section is in units of Mb (10^{-18} cm^2/molec.). The cross section in the 180-240 nm region may be affected by the presence of dimer.

Fig. 6. Quantum yield of fluorescence from photodissociative excitation of HCOOH.

Fig. 7. Quantum yield of fluorescence from photodissociative excitation of $HCOOCH_3$.

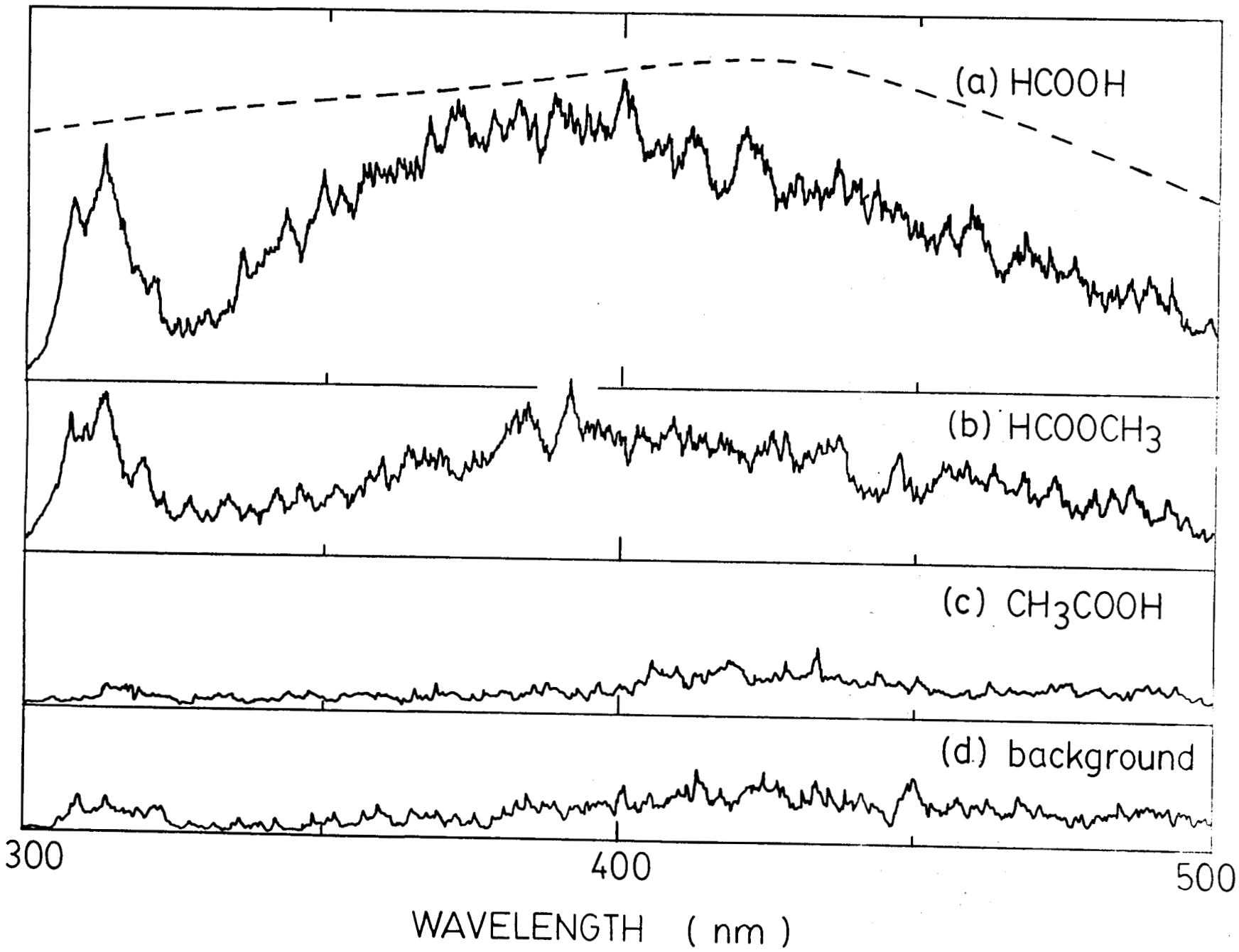
(a) HCOOH
(b) HCOOCH3
(c) CH3COOH
(d) background
300
400
500
WAVELENGTH (nm)

Fig. 1

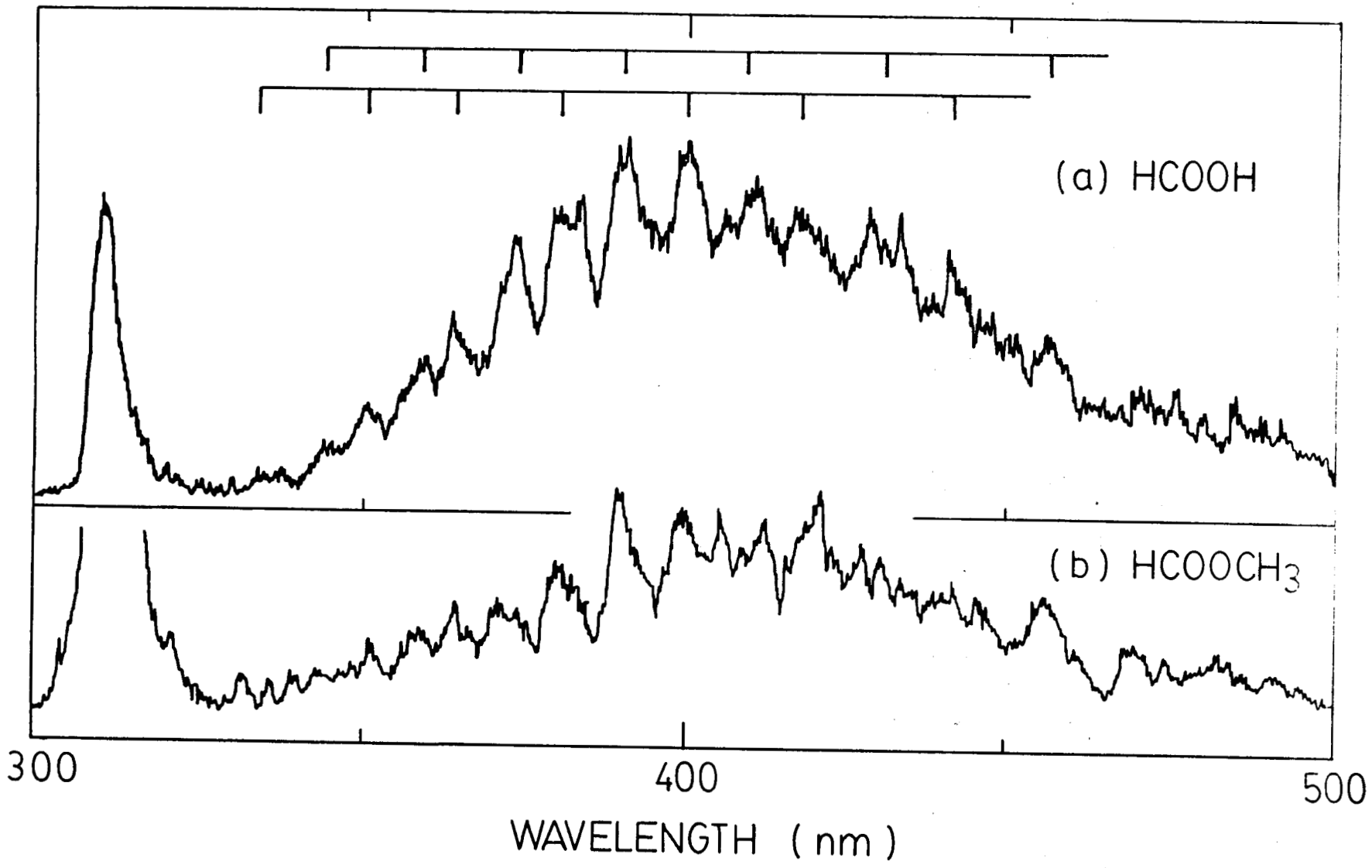

Fig. 2

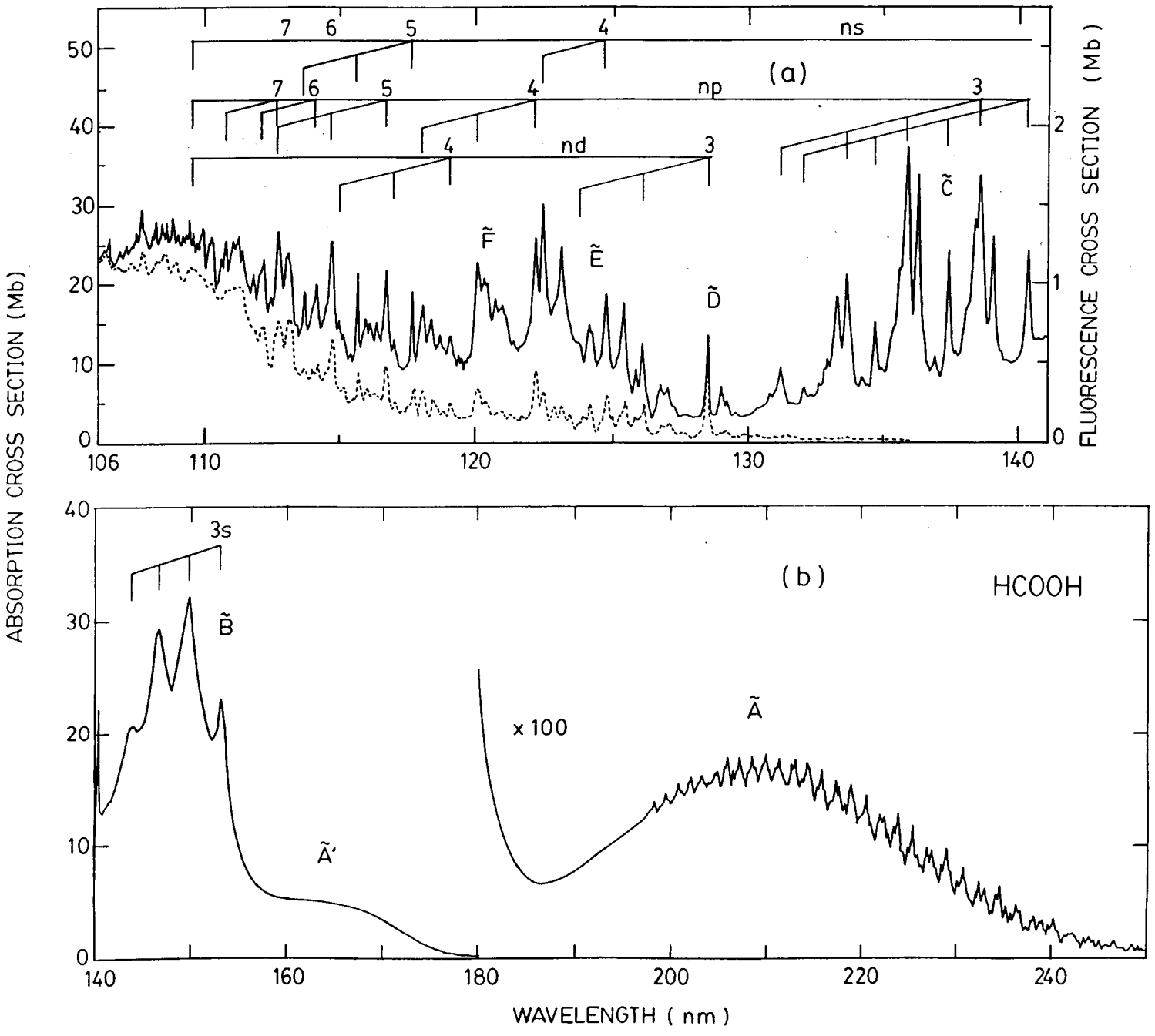
ABSORPTION CROSS SECTION (Mb)
FLUORESCENCE CROSS SECTION (Mb)
WAVELENGTH (nm)
(a)
(b)
HCOOH
ns
np
nd
3s
7 6 5 4
7 6 5 4
4 3
3
C̃
F̃
Ẽ
D̃
B̃
Ã'
Ã
x 100

Fig. 3

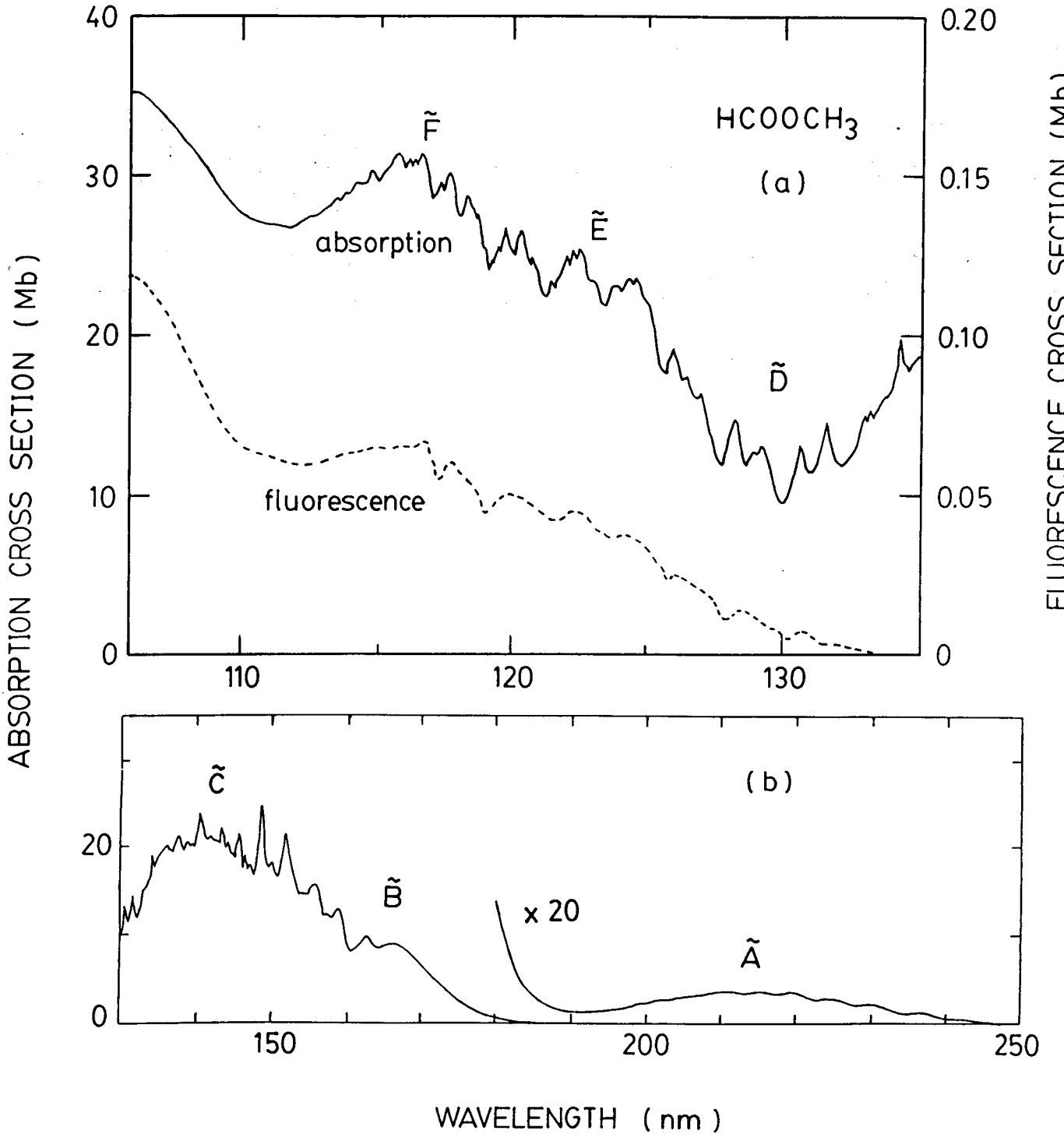
HCOOCH3
(a)
absorption
fluorescence
F̃
Ẽ
D̃
C̃
B̃
Ã
x 20
(b)
ABSORPTION CROSS SECTION (Mb)
FLUORESCENCE CROSS SECTION (Mb)
WAVELENGTH (nm)
40
30
20
10
0
0.20
0.15
0.10
0.05
0
110
120
130
150
200
250

Fig. 4

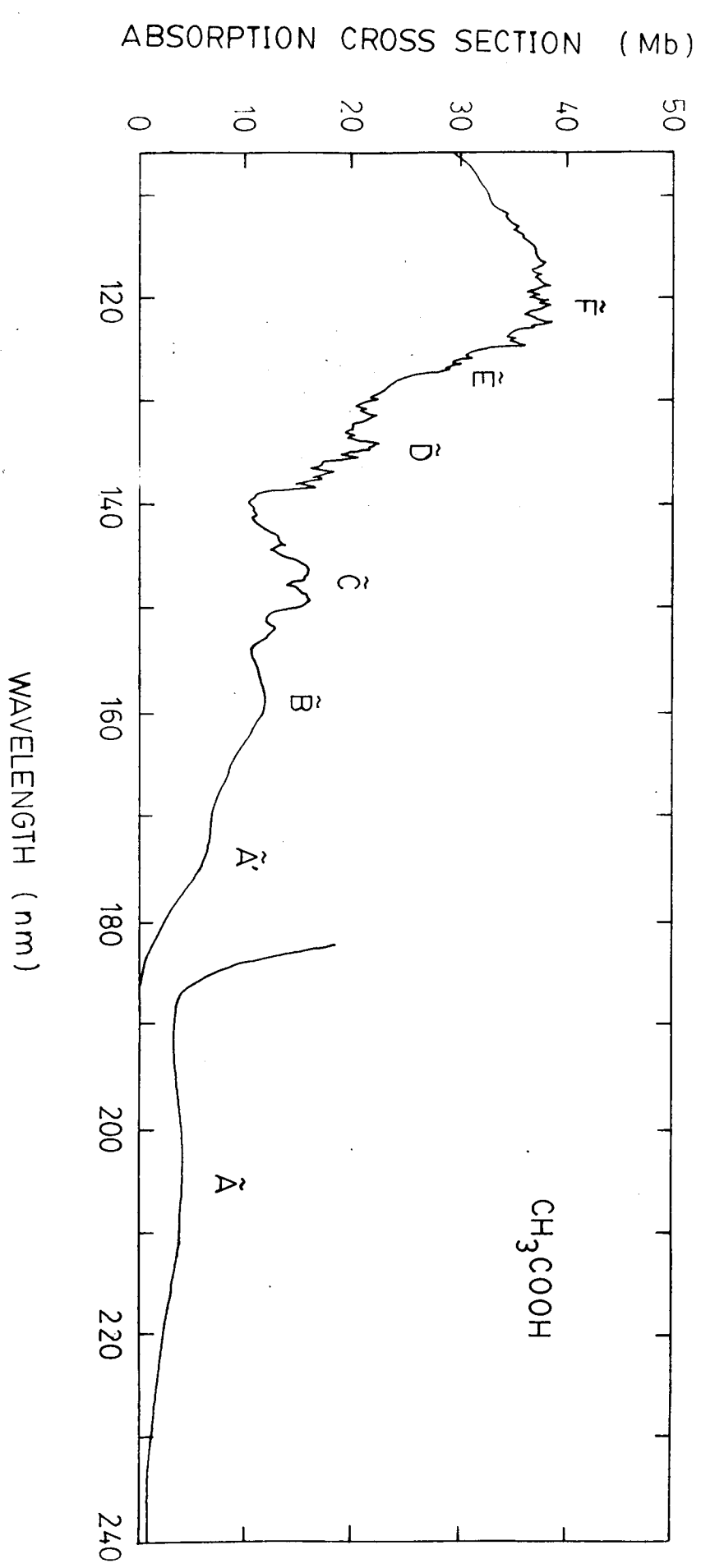
ABSORPTION CROSS SECTION (Mb)
0
10
20
30
40
50
120
140
160
180
200
220
240
WAVELENGTH (nm)
F̃
Ẽ
D̃
C̃
B̃
Ã
X̃
CH3COOH

Fig. 5

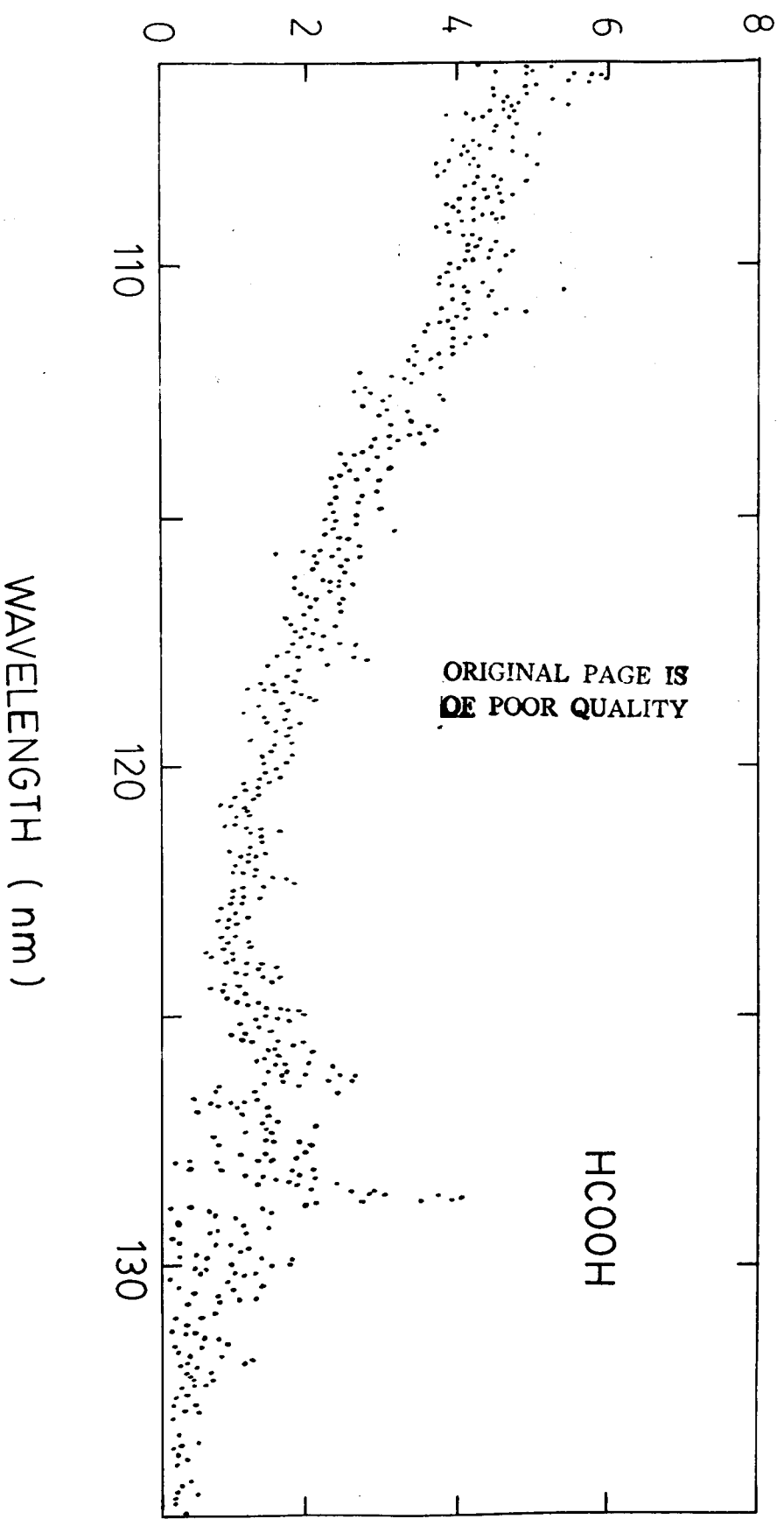
QUANTUM YIELD (%)
0
2
4
6
8
110
120
130
WAVELENGTH (nm)
HCOOH
ORIGINAL PAGE IS
OF POOR QUALITY

Fig. 6

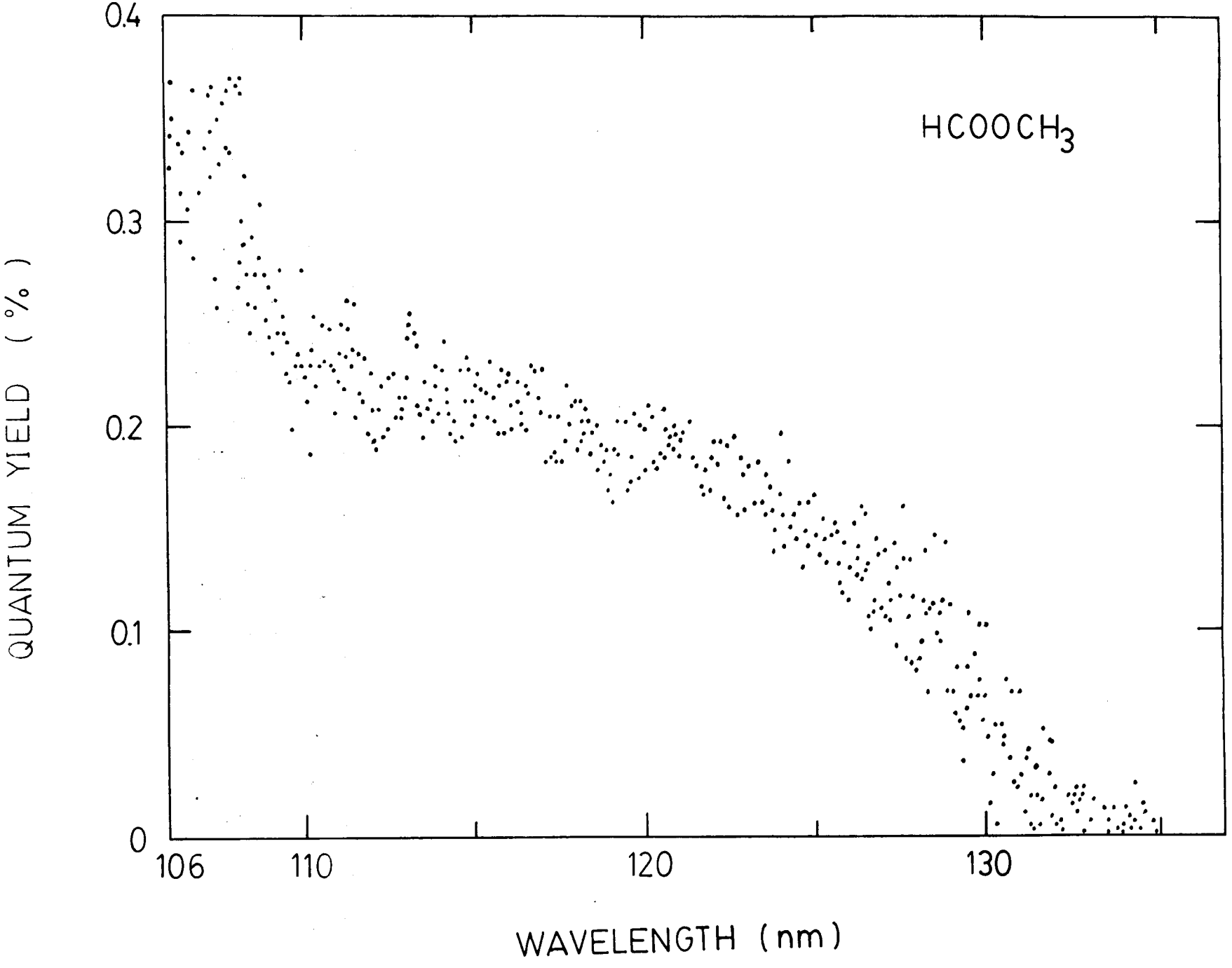
0.4
0.3
0.2
0.1
0
QUANTUM YIELD (%)
HCOOCH3
106
110
120
130
WAVELENGTH (nm)

Fig. 7

Appendix D

CH(A-X, B-X) Emissions from Photodissociative Excitation of CH_3

CH(A-X, B-X) Emissions from Photodissociative Excitation of CH_3

Chao Ye, Masako Suto[a] and L. C. Lee[b]

Department of Electrical and Computer Engineering
San Diego State University
San Diego, California 92182

ABSTRACT

$CH(A^2\Delta, B^2\Sigma^- - X^2\Pi_r)$ emissions were produced by a single-photon excitation of CH_3 at 157.5 nm and a two-photon excitation process at 193 nm. No emissions were detected at 248 nm. The emission intensity from CH_2 is quite small when compared with CH. The CH_3 radicals were produced by the Cl + CH_4 and F + CH_4 reactions as well as by photolysis of methyl compounds. The emission source was identified by modeling the reaction kinetics of the Cl + CH_4 system. Photodissociation process for the absorption continua of CH_3 is discussed.

a) To whom correspondence should be addressed.

b) Also, Department of Chemistry, San Diego State University

I. INTRODUCTION

Methyl radical is an active chemical species involved in hydrocarbon combustion, atmospheric methane oxidation cycle[1], and interstellar molecule formation process[2]. Recently, it is also found that CH_3 radical could lead to formation of diamond film[3]. The spectroscopic information of CH_3 is of interest for these applications and for the fundamental study of photodissociation process as well.

CH_3 has been extensively studied in vacuum ultraviolet (VUV) and ultraviolet (UV) absorption[4,5], photoelectron spectra[6,7], photoelectron detachment[8], and infrared absorption[9]. Molecular orbitals, excited states and molecular geometry of CH_3 are theoretically investigated by many authors[10-14]. Excited states that are optically-forbidden for a single-photon excitation were recently revealed by a resonance-enhanced multiphoton-ionization method[15-21].

Up to now, the VUV spectroscopic studies of CH_3 are limited to Rydberg states[22]. The absorption continua that have a mixed character of Rydberg and valence transitions[23] are very little studied. The existence of absorption continua is evident by the fact that all absorption bands are diffuse[4,5]. Excitation to absorption continua could lead to excited photofragments that consequently emit. Theoretical aspect of the CH_3 photochemistry has been discussed by Yu et al.[14]; but experimental data are

clearly needed for a better understanding of the photodissociation process.

Emissions from excited photofragments could be used as a sensitive means for the detection of CH_3. This photofragment method has been demonstrated in the detection of the HO_2 radical[24-26]. One of the possible applications is for the measurement of reaction kinetics. The reaction kinetics of CH_3 have been measured by the UV[27] and VUV[28] absorption methods. It is expected that better detection sensitivity and spatial resolution will be achieved by the photofragment detection. Since CH_3 does not emit, it can not be detected by the laser-induced-fluorescence technique.

II. EXPERIMENTAL

The experimental apparatus is shown in Fig. 1. A typical discharge flow reactor[24-26] was used to produce methyl radicals by abstraction of hydrogen from CH_4 by halogen atoms (F or Cl), which were produced by microwave discharge of a trace of F_2 in He in an alumina tube or Cl_2 in He in a glass tube. The flow reactor was a Pyrex tube of 1 inch O.D. and 30 cm long coated with Teflon. CH_4 in He was introduced through a movable inlet. Total pressure in the reactor was typically about 2 Torr, and the flow velocity was set at 1000-1500 cm/s.

The gas cell was a six-way stainless steel cross of 4 inch O.D. with a MgF_2 window placed in front of the excimer laser. High purity nitrogen gas continuously flushed between the laser

and gas cell windows for the transmission of VUV light. Laser power was monitored through a sapphire window in the rear side of the gas cell. The window surfaces inside the gas cell were constantly flushed by He to prevent deposition of CH_x radicals on the surfaces. The excimer laser (Lumonics TE860-4) was operated at a repetition rate of 20 Hz (pulse duration of 6 ns). The laser beam was not focused.

Fluorescence was observed through a fused quartz window in a direction perpendicular to the laser beam. The fluorescence was dispersed by an 0.25 m spectrometer (Jarrel-Ash) and detected by a 1024 channel diode array (OMA III, EG&G PARC). Sampling gates opened 1 to 10 μs after each laser pulse. Occasionally, the fluorescence was dispersed by an 0.5 m monochromator (Acton) and the output from a cooled photomultiplier tube (PMT, EMI9558QB) was processed by a boxcar integrator (EG&G, PARC). Emission spectra obtained by these different detection systems are all similar. Emission spectra were taken at varied gas concentrations, laser powers and reaction times. A spectrum with a good signal to noise ratio was typically obtained by an accumulation of 2000 laser shots.

The ArF (193 nm) and KrF (248 nm) laser power was monitored by a power meter (Scientech). The relative power of the F_2 laser (157.5 nm) was monitored by measuring the fluorescence intensity from photodissociation of C_2F_3Cl. At 157.5 nm, C_2F_3Cl dissociates[29] into excited $CFCl^*$ which then emits. C_2F_3Cl flowed slowly with a constant pressure of about 0.2 Torr in a gas cell

separated from the main chamber by a sapphire window. Both C_2F_3Cl and CH_3 simultaneously excited by the same laser beam. The fluorescence from CFCl* was detected by a PMT (EMI 9635 QB) with a band pass filter, and the signal was processed by a boxcar integrator.

In the photolysis experiment, liquid sample of $(CH_3)_2SO$ was kept in a stainless container and degassed at liquid nitrogen temperature. Sample of CH_3Cl, CH_3Br or $(CH_3)_2SO$ with He buffer gas was continuously fed into the gas cell and pumped by a mechanical pump with a cold trap. Pressure in the gas cell was monitored by a capacitance manometer (MKS Baratron).

III. RESULTS

1. CH_3 from the Cl + CH_4 Reaction

CH_3 can be produced by the reaction,

$$Cl + CH_4 \longrightarrow CH_3 + HCl \qquad (1)$$

The reaction rate constant is about 1.0×10^{-13} cm^3 $molec^{-1}s^{-1}$ at 298 K[30]. Chemiluminescence was produced from the reaction. Some chemiluminescence bands can be assigned to the CH, Cl_2 and HCl emissions; however, the source for the chemiluminescence is not clear. Chemiluminescence intensity decreases rapidly with increasing reaction time. The interference of the observed fluorescence by chemiluminescence can be minimized by changing the reaction time. The interference is further avoided by gating the detection system. It is noted that the CH(A-X) band does not appear in the chemiluminescence spectrum.

1.a. Excitation of CH_3 at 157.5 nm

When the reaction medium containing CH_3 was irradiated by F_2 laser photons, fluorescence was observed as shown in Fig. 2. The emission was observed within 10 μs after each laser pulse. This gated detection achieves that the emission is correlated with the laser pulse and the contribution of chemiluminescence is negligible. The emissions at 390 and 431 nm are identified as the CH(B-X) (0,0) and the CH(A-X) (0,0) bands, respectively. The broad band with peak at 490 nm may be partly due to the CH(A-X) (0,1) transition.

The laser power dependence of the CH(A-X) emission intensity is shown in Fig. 3. The slope of the plot is approximately 1, indicating that the fluorescence is produced by a single-photon excitation process. When the laser power was high, noticeable deviation from the straight line was observed as shown in Fig. 2. Additional emission source is evident, which is likely due to the two-photon excitation of secondary reaction products (for example, CH_3Cl[31] as discussed later). When reactant concentrations were limited low, the deviation from a straight line disappeared because of negligible secondary reaction products. No emission was observed from photolysis of CH_4 alone due to extremely small absorption cross section at 157.5 nm[32].

The emission source was investigated by observing the fluorescence intensity at $[Cl_2]$ varied in 0-5 mTorr and $[CH_4]$ in 5-40 mTorr. $[Cl_2]$ was always kept much smaller than $[CH_4]$. The

dependence of fluorescence intensity on [CH_4] is shown in Fig. 4. The fluorescence intensity increases with low [CH_4] and then saturates at high [CH_4]. The dependence of fluorescence intensity on reaction time is shown in Fig. 5. The fluorescence intensity increases with increasing [Cl_2] (or [Cl]). The fluorescence intensity was normalized against the laser power that decreased in the course of experiment. The fluorescence intensity reaches a maximum within 3-6 ms and then decreases at the long reaction time. This decrease indicates that fluorescence arises from transient species (which is likely the CH_3 radical, a primary product of the Cl+CH_4 reaction). The other primary product, HCl, absorbs laser light with an absorption cross section[33] of 3.2×10^{-18} cm^2, but it dissociates into H + Cl so that it does not fluoresce.

In order to check whether the CH_3 radical is indeed the emission source, the concentrations of reaction products were simulated using a Gear routine that solves the simultaneous reaction rate equations[34]. The reactions involved in the modeling are listed in Table I. The wall loss rate (Equation (4) in Table I) was adjusted to best fit the observed fluorescence data shown in Fig. 5. The reaction of Cl + CH_3 $\longrightarrow$ CH_2 + HCl is not considered, because it is an endothermic process such that this reaction does not occur. The loss of CH_3 due to reaction with CH_4 is ignored, because the fluorescence intensity was not reduced by adding CH_4 as shown in Fig. 4. The calculated profiles of [CH_3], [CH_3Cl], and [C_2H_6] as a function of reaction

time are illustrated in Fig. 6. Both of [CH_3Cl] and [C_2H_6] increase monotonically with reaction time, but [CH_3] decreases at the long reaction time. These results corroborate with the assertion that the CH_3 radical is the source for the observed fluorescence.

It is noted that [CH_3Cl] is high even at a short reaction time, if [Cl_2] and [CH_4] are high. Thus, it is expected that the CH(A, B-X) emissions from two-photon excitation of CH_3Cl will show up at high laser power. This explains the additional fluorescence at high laser power as shown in Fig. 3. The fluorescence produced by two-photon excitation of CH_3Cl will be further discussed later. Although [CH_3Cl] is higher than [CH_3], the probability of the two-photon excitation is expected to be small at low laser power so that the observed fluorescence is mainly from CH_3 (see Fig. 3).

The fluorescence cross section can be estimated by comparing the fluorescence intensity with that of C_2F_3Cl, for which the fluorescence cross section is 6×10^{-18} cm^2 at 157.5 nm[29]. If we assume that 10% of Cl_2 is dissociated by the microwave discharge, then [Cl] is in the order of 10^{13} cm^{-3}, which could be mostly converted into [CH_3]. With this assumption, the fluorescence cross section of CH_3 is roughly estimated to be in the order of 10^{-18} cm^2.

The branching ratio for the fluorescence cross sections of CH(B-X) to CH(A-X) is about 8%. The CH_2 ($\tilde{b}$-$\tilde{a}$) emission system may exist in the continuum background shown in Fig. 2; however,

the identification of this emission system is difficult, because the continuum may consist of other emission systems, for example, the CH(A-X) (0,1) band. The branching ratio for the fluorescence cross sections of CH_2 to CH is estimated to be less than 10%, assuming that a half of the continuum background belongs to the CH_2 system. The CH_2 system may in fact be negligibly small.

1.b. Excitation of CH_3 at 193 nm and 248 nm

When the Cl + CH_4 reaction medium was irradiated by ArF laser photons, CH(A, B-X) emissions were observed. The fluorescence spectrum is very similar to that of F_2 laser excitation (Fig. 2). The dependencies of the CH(A-X) fluorescence intensity on reaction time and laser power are shown in Fig. 7 (a) and (b), respectively. The reaction time dependencies are very similar to those observed in the 157.5 nm excitation (Fig. 5); thus, it indicates that the CH emission associates with CH_3. The fluorescence intensity depends on the square of the laser power (I^2), indicating that the CH(A, B-X) emissions are produced by two-photon excitation process.

Photofragment emission from the Cl + CH_4 reaction medium was also studied using an Xe resonance lamp (147 nm) and an KrF laser (248 mn) as light sources. No emission was observed from excitation of the reaction medium by KrF laser photons. When the Xe lamp was used, the OMA was set in the CW mode. The observed signal was too weak to distinguish from chemiluminescence. Thus, the presence of photofragment emission at 147 nm is not certain.

2. CH_3 Produced by the F + CH_4 reaction

CH_3 radicals were also produced by the reaction,

$$F + CH_4 \longrightarrow CH_3 + HF \qquad (2)$$

In this reaction, chemiluminescence was observed only at very short reaction time. The chemiluminescence spectrum consists of the CH(A, B-X), C_2 Swan bands, and HF vibrational-rotational bands as reported previously[35,36].

When the reaction medium was irradiated by F_2 laser photons, the CH(A, B-X) emissions were observed. The fluorescence spectrum (with a resolution of 0.3 nm) for the CH(A-X) emission is shown in Fig. 8. The branching ratio of the CH(A-X) to CH(B-X) emission is similar to that of the Cl+CH_4 reaction medium. When [CH_4] is excess over [F_2], the fluorescence intensity increases linearly with [F_2]. The shorter the reaction time, the stronger is the fluorescence intensity. This reflects the fact that the reaction (2) is very fast (k_2 = 8 x 10^{-11} $cm^3 molec^{-1} s^{-1}$)[36]. The laser power dependence shows that the fluorescence arises from a single-photon excitation process. These results indicate that the CH fluorescence arises from the primary product of the F + CH_4 reaction, namely, CH_3. This confirms the results obtained from the Cl + CH_4 reaction.

When [F] is comparable with [CH_4], the secondary reaction,

$$F + CH_3 \longrightarrow CH_2 + HF \qquad (3)$$

will take place. The CH_2 radical may then be dissociated into CH* + H by a 157.5 nm photon to produce the observed CH fluorescence. Since this process requires two consecutive F

reactions, the fluorescence intensity will be proportional to $[F]^2$ or $[F_2]^2$. This is different from our observation that the CH emission intensity increases approximately linearly with $[F_2]$; thus, the emission source is not produced by the secondary reaction process, that is, CH_2 is not the major emission source. Also, [F] and $[CH_3]$ are more than two order of magnitude smaller than $[CH_4]$ in our experiment, so the $[CH_2]$ produced by reaction (3) is expected to be quite small; therefore, the contribution of CH_2 to the observed CH fluorescence should not be large.

3. CH_3 produced by Photolysis of Methyl Compounds

Production of CH_3 by photolysis of methyl compounds, CH_3Cl, CH_3Br, and $(CH_3)_2SO$, was also investigated in this experiment. When CH_3Cl is irradiated by F_2 laser photons, product of CH_3 and Cl is likely the major channel. CH_3 may then be excited by another photon to produce CH emissions, namely,

$$CH_3Cl + h\nu\ (157.5) \longrightarrow CH_3 + Cl, \qquad (4)$$

$$CH_3 + h\nu\ (157.5) \longrightarrow CH^* + H_2. \qquad (5)$$

The CH(A, B-X) emissions by photoexcitation of CH_3Cl at 157.5 nm are shown in Fig. 9 (a) and also a higher resolution spectrum in Fig. 9 (b). The emission intensity depends linearly on $[CH_3Cl]$ and quadratically on laser power shown in Fig. 9 (c). These results are consistent with the attribution of stepwise excitation (4) and (5) to the observed CH fluorescence. The probability for the process that one photon dissociates CH_3Cl into CH_2Cl + H and another photon dissociates CH_2Cl to produce CH emissions is expected to be small, because the CH_2Cl-H bond is

stronger than the CH_3-Cl bond. However, the contribution of this process is not totally ruled out.

The CH(A, B-X) emissions were observed from photoexcitation of CH_3Cl by ArF laser photons at 193 nm. The laser power dependence of the emission intensity indicates that the excitation is a two-photon excitation process. The CH(A, B-X) emissions were commonly observed by the two-photon excitation of CH_3X (X=Br, I and OH) with ArF laser photons[37-39]. Baronavski and McDonald[38] suggested that the fluorescence from photoexcitation of CH_3Br is by,

$$CH_3Br + h\nu(193) \rightarrow CH_3^{\ddagger} + Br, \qquad (6)$$

$$CH_3^{\ddagger} + h\nu(193) \rightarrow CH^* + H_2. \qquad (7)$$

High vibrational energy is required for process (7) to occur. On the other hand, Fotakis et al.[39] favored the simultaneous two-photon excitation,

$$CH_3X + 2h\nu\ (193) \rightarrow CH_3X^{**} \rightarrow CH^* + H_2 + X. \qquad (8)$$

The probability for this simultaneous excitation may be smaller than the stepwise excitation, because CH_3X^{**} has an excitation energy of 12.8 eV that will mostly lead to ionization.

No emission was observed from the multiphoton excitation of CH_3Cl at 248 nm. CH_3Cl has a very small absorption cross section at 248 nm[40], so the two-photon excitation coefficient is expected to be small. Also, there is no emission from the 248 nm excitation of CH_3; thus, the chance for stepwise excitation is eliminated.

The CH(A, B-X) emission was observed when CH_3Br was irradiated by F_2 laser photons. The absorption cross section of CH_3Br at 157.5 nm[41] is about 6×10^{-19} cm^2. The absorption is a continuum, so the excited molecules undergo dissociation. The CH emission intensity is proportional to $[CH_3Br]$ and quadratically dependent on laser power. These results suggest that the excitation is a two-photon process. Similar to CH_3Cl, the excitation is likely a two-step photodissociation process. When the gate was left off, Br_2 emissions[42] were observed. The Br_2 emissions are likely due to the secondary reaction,

$$Br + Br\ (+M) \longrightarrow Br_2^*\ (+M). \qquad (9)$$

Emission from photoexcitation of $(CH_3)_2SO$ at 157.5 nm was also examined, because this compound is often used as a methyl radical source[15-18]. The CH(A, B-X) emissions were observed. The emission intensity depends linearly on $[(CH_3)_2SO]$ and quadratically on laser power. These results indicate that the CH emission is produced by the two-photon excitation process,

$$(CH_3)_2SO + h\nu\ (157) \longrightarrow CH_3 + CH_3SO, \qquad (10)$$

$$CH_3 + h\nu\ (157) \longrightarrow CH^* + H_2. \qquad (5)$$

IV. Discussion

The current excitation wavelengths do not coincide with any Rydberg states[4,5,18]; therefore, the observed fluorescence is produced by dissociative states. These dissociative states are expected, because the Rydberg states are very diffuse[4,5]. However, the nature of the dissociative continua is not yet

studied, and the current observations provide information for such study.

4.a. Rydberg states and Dissociation Limits

It is well established[14,17,22] that the ground electronic state of CH_3 is of D_{3h} symmetry with an electron configuration,

$$(1a_1')^2(2a_1')^2(1e')^4(1a_2'')^1,\ \tilde{X}^2A_2''.$$

The optically-allowed transitions for excitation of the $1a_2''$ orbital to various Rydberg orbitals were observed[4,5] at 216.0, 150.3, 149.7, and 140.8 nm for the $\tilde{B}$, $\tilde{C}$, $\tilde{D}$ and $\tilde{E}$ states, respectively. Optically-forbidden transitions were observed by two-photon excitation, in which the 3p orbital was determined at 7.43 eV[17,18]. The potential energies of these Rydberg states are indicated in Fig. 10. Herzberg[5] pointed out that the first excited state, $\tilde{B}\ ^2A_1'$, should dissociate into $CH_2(\tilde{X}^1A_1') + H(^2S)$. Danon et al.[19] measured the lifetime of the $\tilde{B}$ state to be 0.12 ps using a multiphoton ionization technique.

Energy threshold is an essential information needed for understanding the photoexcitation process. The energy thresholds for various dissociation processes can be calculated from the enthalpy changes, for example, the enthalpy changes for the dissociation processes,

$$CH_3 \longrightarrow CH_2 + H, \qquad (11)$$

$$\longrightarrow CH + H_2, \qquad (12)$$

are ΔH=109.6 kcal/mol for (11) and 107.1 kcal/mol for (12), using the thermochemical values of JANAF Table[43]. Taking the excitation energies for the excited $CH(A^2\Delta$ and $B^2\Sigma^-)$ states to be

2.875 and 3.229 eV[44], the energy thresholds for the production of the CH(A-X) and CH(B-X) emissions by photoexcitation of CH_3 are 7.53 and 7.88 eV, respectively. Photoexcitation of CH_3 could also produce the $CH_2(\tilde{b}^1B_1 - \tilde{a}^1A_1)$ and $CH_2(\tilde{c}^1A_1 - \tilde{a}^1A_1)$ emissions. The $\tilde{a}$ state is about 0.5 eV[45] above the ground electronic state ($\tilde{X}^3B_1$). The energies required to produce $CH_2(\tilde{b}-\tilde{a})$ and $CH_2(\tilde{c}-\tilde{a})$ emissions by photoexcitation of CH_3 are about 6.2 and 8.7 eV, respectively. These dissociation energy thresholds are indicated in Fig. 10, along with the laser photon energies.

4.b. Photodissociation Processes at 157 nm

As shown in Fig. 10, the F_2 laser photons (which consist three lines at 156.71, 157.48, and 157.59 nm) have energy barely enough to produce the excited species of CH(B), and sufficient energy to produce CH(A) and $CH_2(\tilde{b})$. In this experiment, the CH(A,B-X) emissions were observed, but the presence of the $CH_2(\tilde{b}-\tilde{a})$ emission is not certain. The CH_2 emission spreads widely from 400 nm to infrared, and it could be hidden in the continuum emission background (see Figs. 2, 8 and 9). In any case, the CH_2 emission intensity is much weaker than that of the CH emission. This result differs from the expectation of Yu et al.[14] that the CH + H_2 process is a minor pathway when compared with the CH_2 + H process.

The photoabsorption cross section of CH_3 at 157 nm is not known. Since the CH emission is produced by a single-photon process, the absorption cross section must be sufficiently large. In general, polyatomic molecules have absorption continua

underneath discrete states. The absorption continua usually have mixed character of Rydberg and valence states[23]. The observed CH emissions are produced by direct excitation of CH_3 through these dissociative continua. The absorption cross sections of CH_3 at the Rydberg states of 150.4, 150.0 and 149.7 nm were measured by Pilling et al.[46] and 216 nm by Arthur [27]. The cross sections at the band peaks are high, for example, 4.85×10^{-16} cm^2 at 150.4 nm. Considering such high cross sections for the discrete states, the absorption continua may have a large strength. Taking the estimated fluorescence cross section in the order of 10^{-18} cm^2 and a fluorescence quantum yield of 10% (this value is in the upper side for a typical high fluorescing molecule), the absorption continua could have a cross section in the order of 10^{-17} cm^2. It is of interest to measure the cross section of the absorption continua over a wide wavelength range.

The CH emissions observed from photoexcitation of methyl compounds (CH_3Cl, CH_3Br and $(CH_3)_2SO$) are most likely produced by a stepwise two-photon excitation process. The contribution from the simultaneous two-photon excitation ($CH_3X + 2h\nu(157.5) \longrightarrow CH_3X^{**} \longrightarrow CH^* + H_2 + X$) may be small, because the laser beam is not focused (about 10^{14} photons/cm^2 per pulse) such that the laser flux is not high enough for a strong simultaneous multiphoton excitation. Also, the simultaneous two-photon excitation will excite the molecule up to 15.7 eV where the ionization channel dominates and the fluorescence yield is usually small.

When the CH_3 radical is produced by photodissociation of methyl compounds, it may carry a large amount of kinetic energy and rotational-vibrational energy, depending on the parent molecules. However, the observed fluorescence spectra are very similar for all molecules studied. These results indicate that the emitting species may be all produced by the same dissociative state(s) and/or the fluorescence spectra are limited by the nature of the excited CH states.

4.c. Photoexcitation Process at 193 nm

The CH(A, B-X) emissions were observed from photoexcitation of CH_3 by ArF laser photons. As shown in Fig. 10, the photon energy of 193 nm is not enough to produce the CH emission; thus, the emissions must be produced by multiphoton excitation process. There is no discrete absorption band of CH_3 around 193 nm, so the excitation must go through absorption continua. The absorption spectrum of CH_3 shows absorption continuum in the 210-220 nm region[47], which may extend toward the shorter wavelength.

The dissociation process at 193 nm may be similar to that of 216 nm band[5], that is,

$$CH_3 + h\nu(193) \longrightarrow CH_2(X)^{\neq} + H, \qquad (13)$$

where $CH_2(X)^{\neq}$ indicates vibrational or rotational excited states. The 193 nm light has sufficient energy to produce $CH_2(\tilde{b})$, but emission from this excited species is not well identified. A second photon may further dissociate the CH_2 radical into CH* + H, and consequently emits,

$$CH_2 + h\nu\ (193) \longrightarrow CH^*\ (A,B) + H. \qquad (14)$$

Probability for the simultaneous two-photon excitation,

$$CH_3(\tilde{X}) + 2h\nu\ (193) \longrightarrow CH_3^{**} \longrightarrow CH^*\ (A,B) + H_2, \quad (15)$$

$$\longrightarrow CH^*\ (A,B) + 2H, \quad (16)$$

may be small, because it will excite CH_3 to 12.8 eV, where ionization channel dominates and the fluorescence yield is usually quite small. The probability for the production of the CH emissions by the stepwise excitation,

$$CH_3 + h\nu(193) \longrightarrow CH(X)^{\ddagger} + H_2 \quad (17)$$

$$CH + h\nu(193) \longrightarrow CH^* \quad (18)$$

is also expected to be small, because there are no CH resonance states at 193 nm.

The spectral profiles of the CH emissions are always about the same, in spite of different excitation wavelength and excitation process. This similarity may be inherent with the nature of the CH excited states. The high rotational and vibrational levels are predissociated[44] so that the emission is only due to the low rotational levels of the CH(A,B) v=0 vibrational levels that produce similar emission spectra.

4.d. Photoexcitation at 248 nm

No emissions were detected at 248 nm excitation. The KrF laser power is a factor of 2-3 stronger than the ArF laser; thus the KrF laser must have a high multiphoton excitation efficiency if CH_3 has similar photoabsorption cross sections at both wavelengths. The non-emission indicates that the absorption cross section of CH_3 at 248 nm must be very small.

V. CONCLUDING REMARKS

Photoexcitation process of methyl radicals produced by the reactions of Cl + CH_4 and F + CH_4 is studied using excimer lasers as light sources. The CH(A, B - X) emissions are produced by a single-photon excitation process at 157.5 nm. The emission source is confirmed by the dependencies of emission intensity on reactant concentrations and reaction time. The fluorescence cross section was estimated to be in the order of 10^{-18} cm^2. The CH emissions are produced by two-photon excitation of CH_3 at 193 nm. No emissions were detected at 248 nm. Our results indicate that the absorption continua have large cross sections at 157.5 and 193 nm, but not 248 nm. Measurements for the cross sections of the absorption continua are of interest for further study of photodissociation process.

ACKNOWLEDGEMENT

The authors wish to thank M. C. Lin at Naval Research Laboratory for useful discussion and suggestions. They also thank D. Coffey, Jr. at San Diego State University for providing the computer program for modeling the Cl + CH_4 reaction kinetics. This paper is based on the work supported by the NSF and the NASA.

REFERENCE

1. B. J. Finlayson-Pitts and J. N. Pitts Jr. "Atmospheric Chemistry," (Wiley, New York, 1986)
2. A. Dalgalno and J. H. Black, Rep. Prog. Phys. 39, 573 (1976)
3. Y. Saito, S. Matsuda and S. Nogita, J. Material Sci. Lett. 5, 569 (1986); Y. Hirose and y. Terasawa, Jpn. J. Appl. Phys. 25, L519 (1986); S. Matsumoto, M. Hino, and T. Kobayashi, Appl. Phys. Lett. 51, 737 (1987).
4. G. Herzberg and J. Shoosmith, Can. J. Phys. 34, 523 (1956)
5. G. Herzberg, Proc. Roy. Soc. London Ser. A 262, 291 (1961)
6. J. Dyke, N. Jonathan, E. Lee and A. Morris, J. Chem. Soc. Faraday Trans. 2, 72, 1385 (1976)
7. T. Koenig, T. Balle, and W. Snell, J. Am. Chem. Soc. 97, 662 (1975)
8. G. B. Ellison, P. C. Engelking and W. C. Lineberger, J. Am. Chem. Soc. 100, 2556 (1978)
9. C. Yamada, E. Hirota, K. Kawaguchi, J. Chem. Phys. 75, 5256 (1981)
10. K. Morokuma, L. Pedersen, and M. Karplus, J. Chem. Phys. 48, 4801 (1968)
11. Y. Ellinger, F. Pauzat, V. Barone, J. Douady and R. Subra, J. Chem. Phys. 72, 6390 (1980)
12. G. T. Surratt and W. A. Goddard III, Chem. Phys. 23, 39 (1977)
13. J. Pacansky, J. Phys. Chem. 86, 485 (1982)

14. H. T. Yu, A. Sevin, E. Kassab and E. M. Evleth, J. Chem. Phys. 80, 2049 (1984)

15. T. G. DiGiuseppe, J. W. Hudgens and M.C. Lin, Chem. Phys. Lett. 82, 267 (1981)

16. T. G. DiGiuseppe, J. W. Hudgens and M. C. Lin, J. Phys. Chem. 86, 36 (1982)

17. J. W. Hudgens, T. G. DiGiuseppe and M. C. Lin J. Chem Phys. 79, 571 (1983)

18. M. C. Lin and W.A. Sanders, Adv. Multiphoton Processes 2, 333 (1986)

19. J. Danon, H. Zacharias, H. Rottke and K. H. Welge, J. Chem. Phys. 76, 2399 (1982)

20. B. H. Rockney and E.R. Grant, J. Chem. Phys. 77, 4257 (1982)

21. P. Chen, S. D. Colson, W. A. Chupka and J. A. Berson, J. Phys. Chem., 90, 2319 (1986)

22. G. Herzberg, "Electronic Spectra of Polyatomic Molecules," Von Nostrand Reinhold, New York, 1966

23. M. B. Robin "Higher Excited States of Polyatomic Molecules," vol. 1 (1974) and vol. 3 (1985), Academic Press, New York.

24. M. Suto and L. C. Lee, J. Chem. Phys. 80, 195 (1984)

25. L. C. Lee, H. Helm and J. S. Chang, Chem. Phys. 81, 537 (1981); L. C. Lee, J. Chem. Phys. 76, 4909 (1982)

26. E.R. Manzanares, M. Suto, L. C. Lee, and D. Coffey, Jr., J. Chem. Phys. 85, 5027 (1986); X. Wang, M. Suto and L. C. Lee, J. Chem. Phys. in press.

41. M. Suto and L. C. Lee, unpublished data.

42. R. W. B. Pearse and A. G. Gaydon, "The Identification of Molecular Spectra," Chapman and Hill, London (1976)

43. M. W. Chase, Jr., C. A. Davies, J. R. Downey, Jr., D. J. Frurip, R. A. McDonald, and A. N. Syverud, "JANAF Thermochemical Tables," Third ed. J. Phys. Chem. Reference Data, 14, (1985) Supplement No. 1.

44. K. P. Huber and G. Herzberg, "Constants of Diatomic Molecules," Van Nostrand Reinhold, New York, 1979

45. J. Romelt, S. D. Peyerimhoff and R. S. Bunker, Chem. Phys. 54, 147 (1981)

46. M. J. Pilling, A. M. Bass and W. Braun, Chem. Phys. Lett. 9, 147 (1971)

47. D. A. Parkes, D. M. Paul, and C. P. Quinn, J. Chem. Soc. Faraday Trans. 1, 72, 1935 (1976).

Table I

Reactions used for modeling the Cl + CH_4 system.

	Reactions	Rate constants[a] (cm^3 $molec^{-1}$ s^{-1})	Ref.
1.	Cl + CH_4 ⟶ CH_3 + HCl	1.0×10^{-13}	30
2.	CH_3 + Cl_2 ⟶ CH_3Cl + Cl	2.0×10^{-12}	31
3.	CH_3 + CH_3 ⟶ C_2H_6	4×10^{-11}	27[b]
4.	CH_3 ⟶ wall loss	(150)[c]	--
5.	CH_3Cl + Cl ⟶ CH_2Cl + HCl	4.9×10^{-13}	30

a. All reaction rate constants are measured at room temperature (298 - 300 K)

b. CH_3 + CH_3 + He ⟶ C_2H_6 + He measured at a total pressure of 4-575 Torr.

c. Value adjusted for best fit to experimental data. The unit is s^{-1}.

Figure Caption

Fig. 1. Schematic diagram for the experimental setup.

Fig. 2. The CH(A,B-X) fluorescence spectrum observed from irradiation of the Cl + CH_4 reaction medium by F_2 laser photons. The partial pressures are: [CH_4] = 50 mTorr, [Cl_2] = 2 mTorr, and [He] = 1.5 Torr. Cl atoms are produced by a microwave discharge of Cl_2 in He. The flow velocity is about 1000 cm/s, and the reaction time is about 3 ms. The spectral resolution is 12 nm, and the OMA gate duration is 10 μs.

Fig. 3. The laser power dependence of the CH (A-X) fluorescence intensity produced from excitation of the Cl + CH_4 reaction medium by F_2 laser photons. The slope of the plot is about 1 at small laser power. Experimental parameters are: [Cl_2] = 1 mTorr, [CH_4] = 15 mTorr, total pressure = 1.9 Torr, flow velocity = 1515 cm/s, and reaction time = 4 ms.

Fig. 4. The CH (A-X) fluorescence intensity produced from excitation of the Cl + CH_4 reaction medium by F_2 laser photons at varied [CH_4]. Experimental parameters are fixed at [Cl_2] = 2.2 mTorr, [He] = 2.2 Torr, and reaction time of about 6 ms.

Fig. 5. The CH(A-X) fluorescence intensity produced from excitation of the Cl + CH_4 reaction medium by F_2 laser photons at varied reaction times. Experimental parameters are: [CH_4] = 20 mTorr, [Cl_2] = 2.1 mTorr, and [He] = 2 Torr

Fig. 6. The simulated concentrations of reaction products, CH_3, C_2H_6, and CH_3Cl, in the Cl + CH_4 reaction medium. The concentrations of [Cl_2] = 2.1 mTorr, [Cl] = 0.1 [Cl_2], and [CH_4] = 20 mTorr, and the reaction rate constants listed in Table I are used in the calculation.

Fig. 7. The reaction time dependence (a) and laser power dependence (b) of fluorescence intensity produced from excitation of the Cl + CH_4 reaction media by ArF laser photons. (a) [Cl_2] = 1 mTorr, [CH_4] = 26 mTorr, and [He] = 1.8 mTorr; (b) [Cl_2] = 1 mTorr, [CH_4] = 15 mTorr, and [He] = 1.8 mTorr at a reaction time of 4 ms.

Fig. 8. The CH (A-X) fluorescence spectrum produced from excitation of the F + CH_4 reaction medium by F_2 laser photons. The emission is dispersed by a 0.5 m monochromator with a resolution of 0.3 nm. Experimental parameters are: [F_2] = 4 mTorr, [CH_4] = 20 mTorr, [He] = 1.5 Torr, and reaction time = 3.5 ms.

Fig. 9. Fluorescence from excitation of CH_3Cl by F_2 laser photons. (a) The CH(A, B - X) emissions with a resolution of 12 nm. (b) The CH(A - X) emission with a resolution of 1.5 nm. (c) laser power dependence of the CH(A - X) emission intensity. The sample gas is 60 mTorr CH_3Cl diluted in 1.1 Torr He.

Fig. 10 Potential energies for the Rydberg States and the dissociation limits of CH_3. Laser photon energies are also indicated.

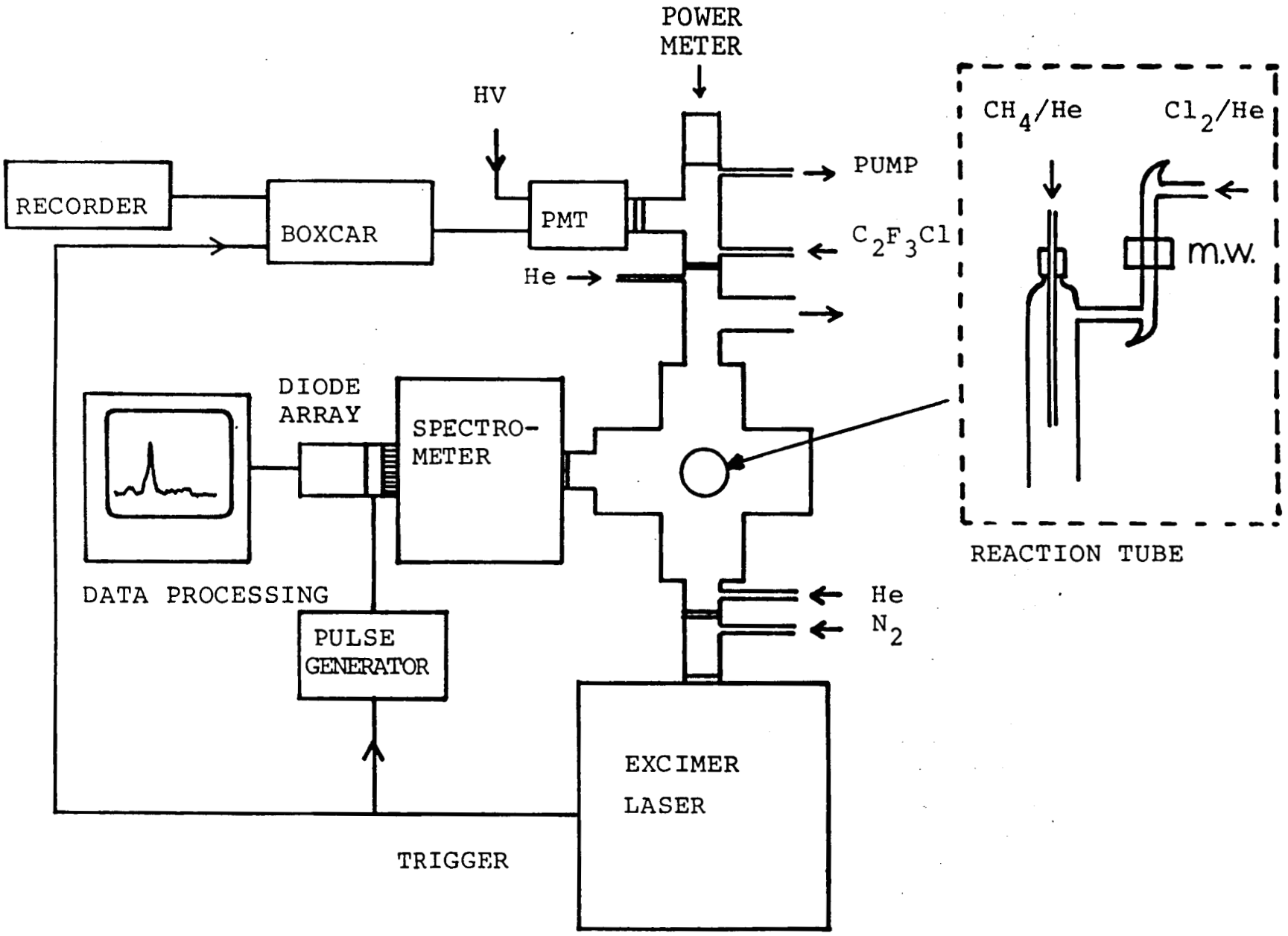
POWER
METER
HV
RECORDER
BOXCAR
PMT
PUMP
C_2F_3Cl
He
CH_4/He
Cl_2/He
m.w.
DIODE
ARRAY
SPECTRO-
METER
DATA PROCESSING
REACTION TUBE
He
N_2
PULSE
GENERATOR
EXCIMER
LASER
TRIGGER

Fig. 1

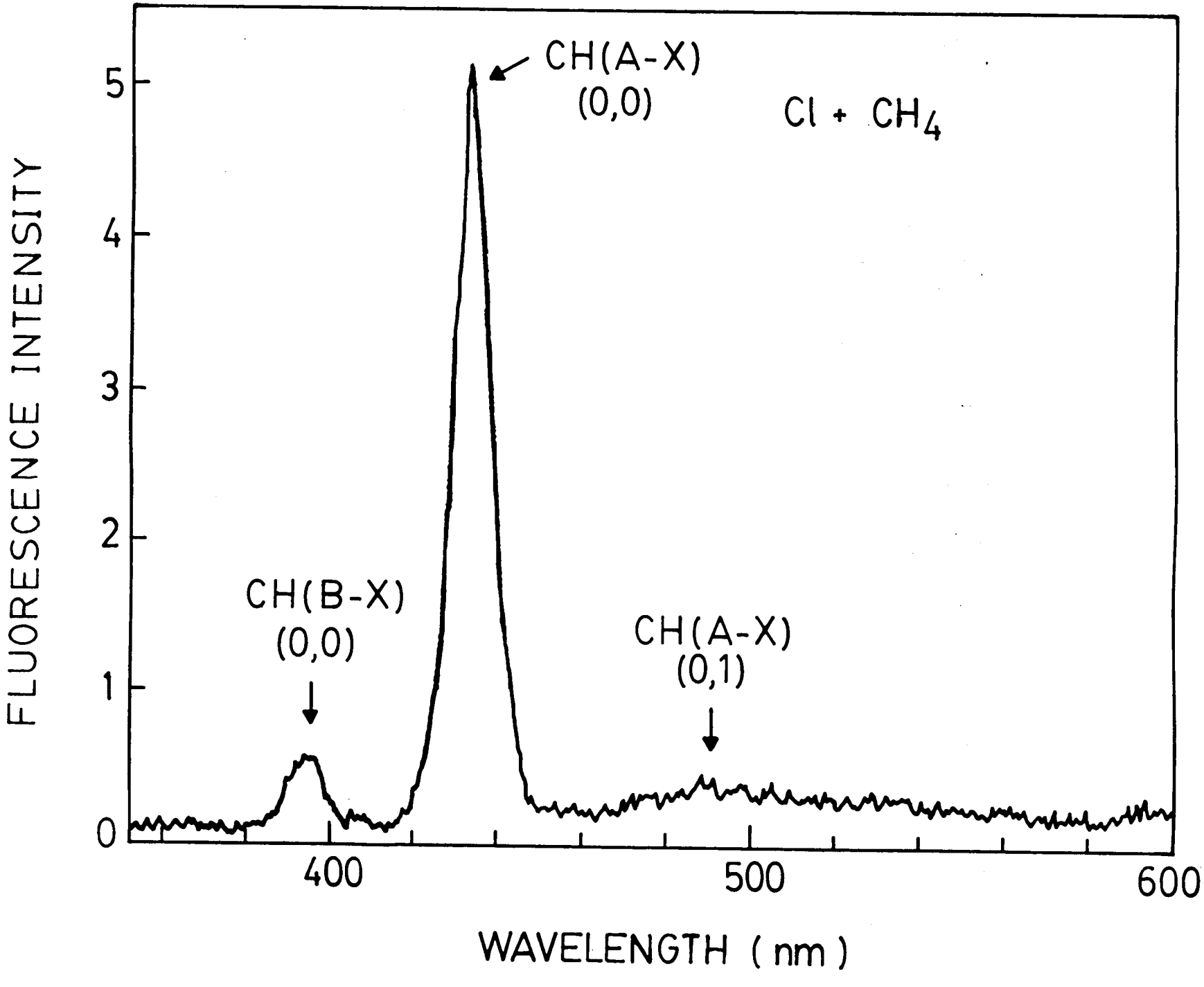
CH(A-X)
(0,0)
Cl + CH4
CH(B-X)
(0,0)
CH(A-X)
(0,1)
FLUORESCENCE INTENSITY
0
1
2
3
4
5
400
500
600
WAVELENGTH (nm)

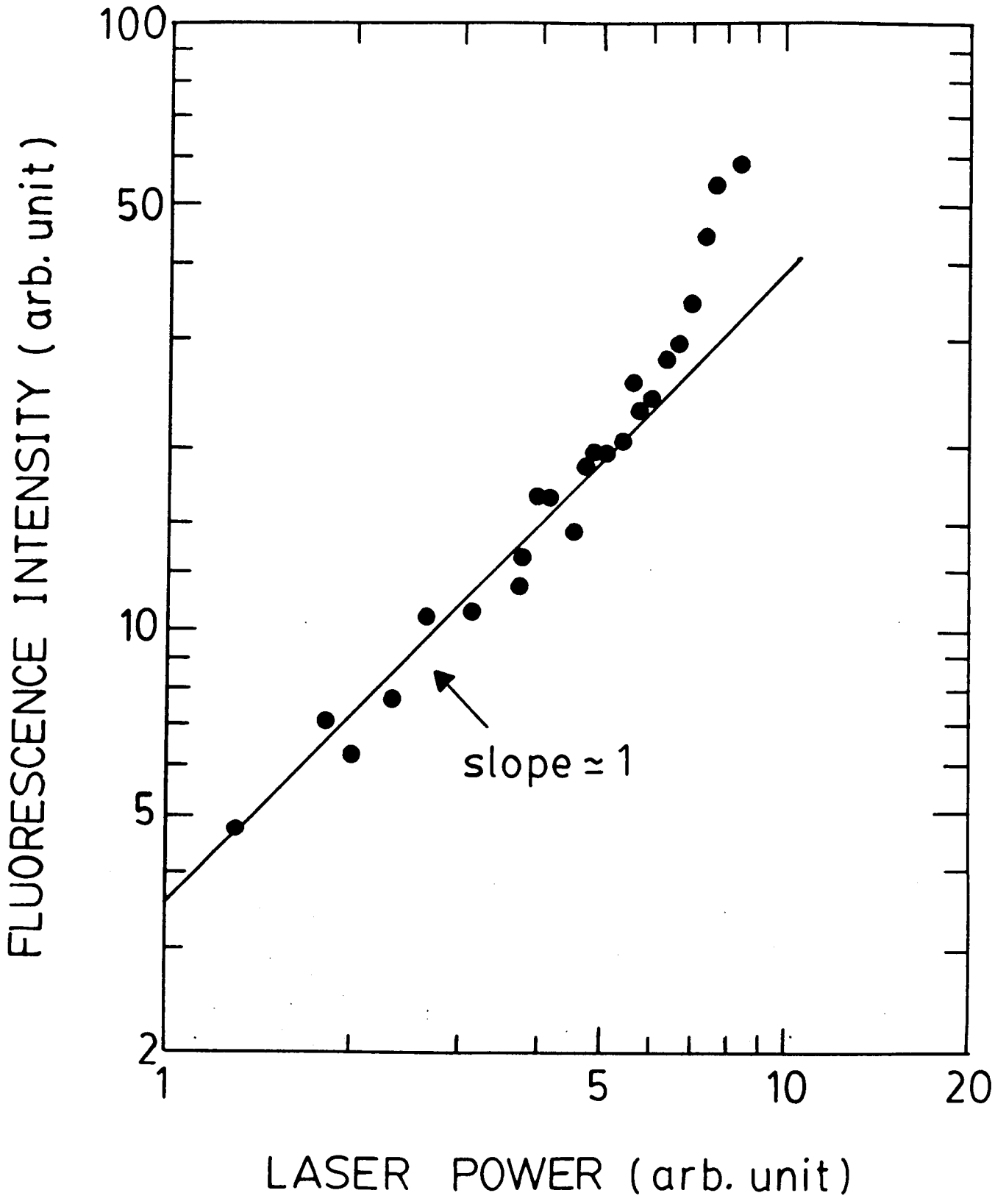
100
50
10
5
2
1
5
10
20
FLUORESCENCE INTENSITY (arb. unit)
LASER POWER (arb. unit)
slope ≃ 1

Fig. 3

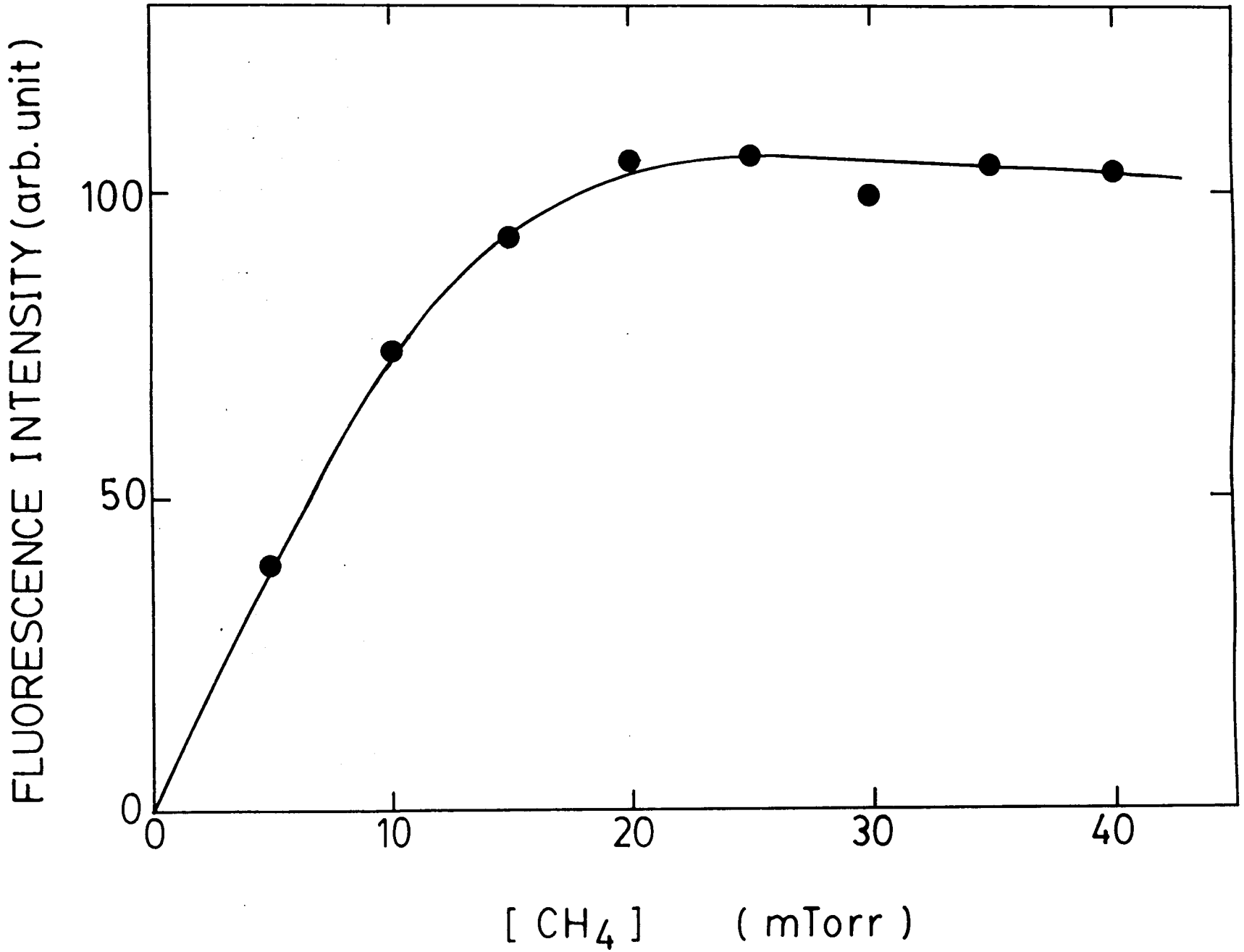
FLUORESCENCE INTENSITY (arb. unit)
100
50
0
0
10
20
30
40
[CH4] (mTorr)

Fig 4

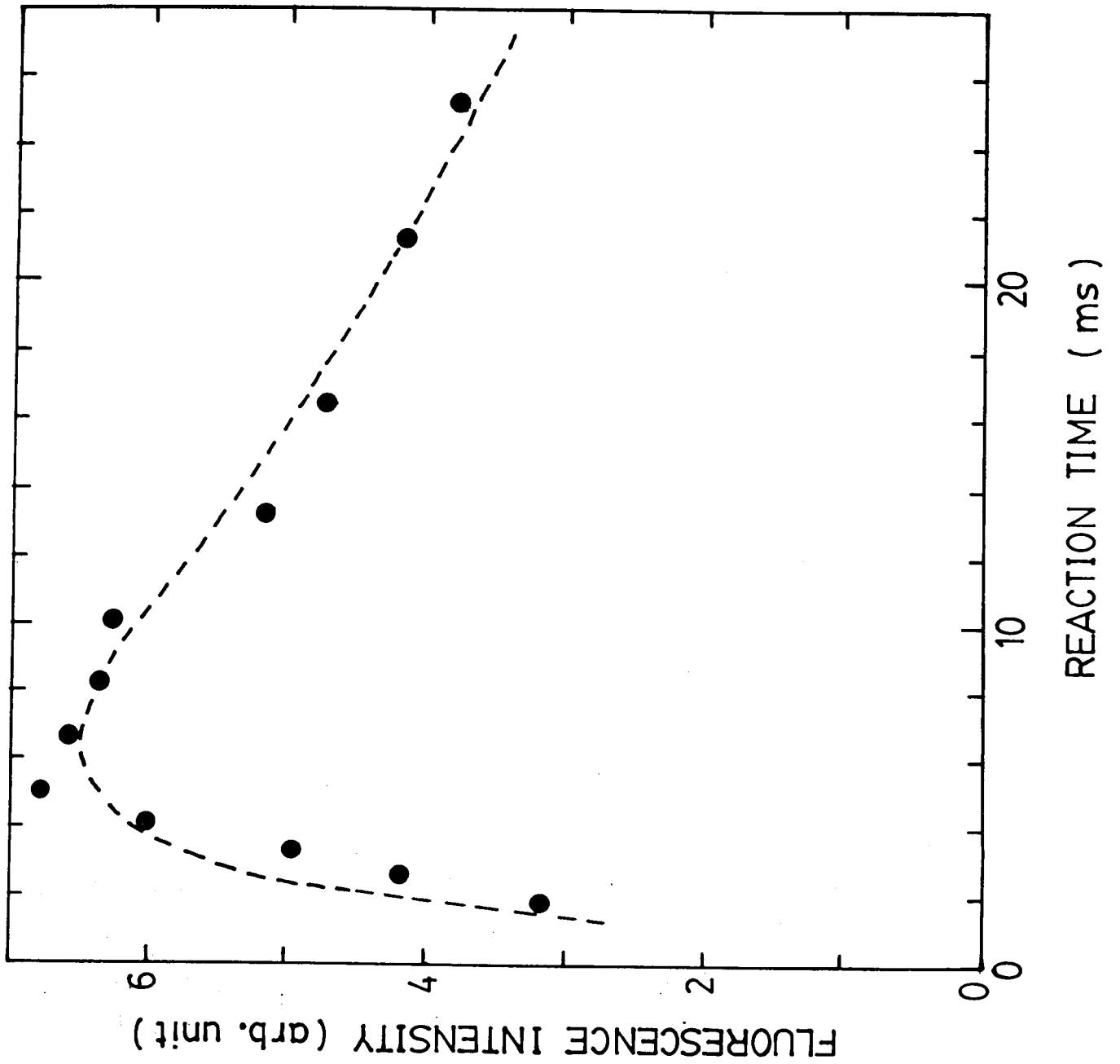
FLUORESCENCE INTENSITY (arb. unit)
0
2
4
6
0
10
20
REACTION TIME (ms)

Fig. 5

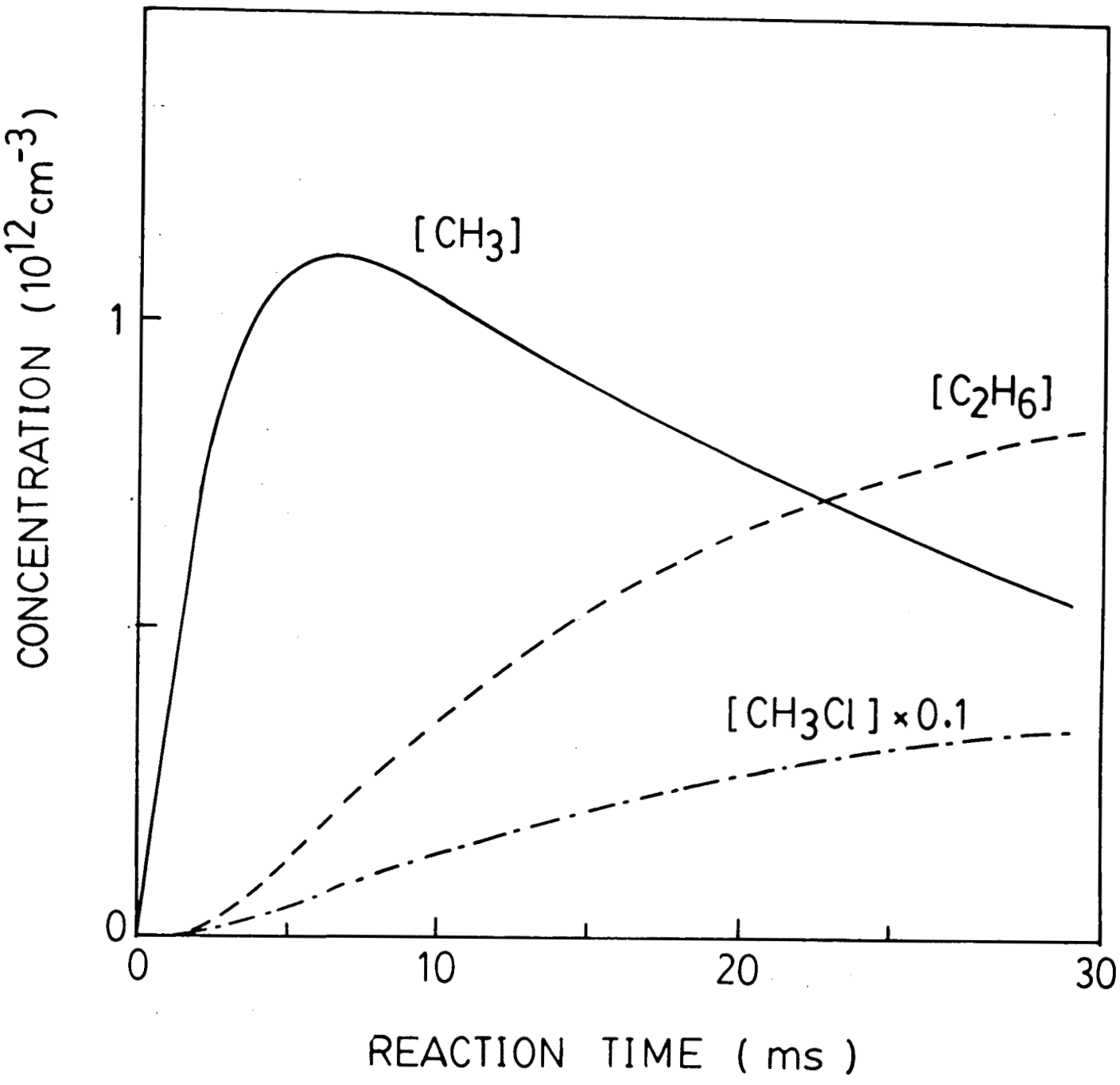
CONCENTRATION ($10^{12}cm^{-3}$)
1
0
[CH_3]
[C_2H_6]
[CH_3Cl] × 0.1
0
10
20
30
REACTION TIME (ms)

Fig. 6

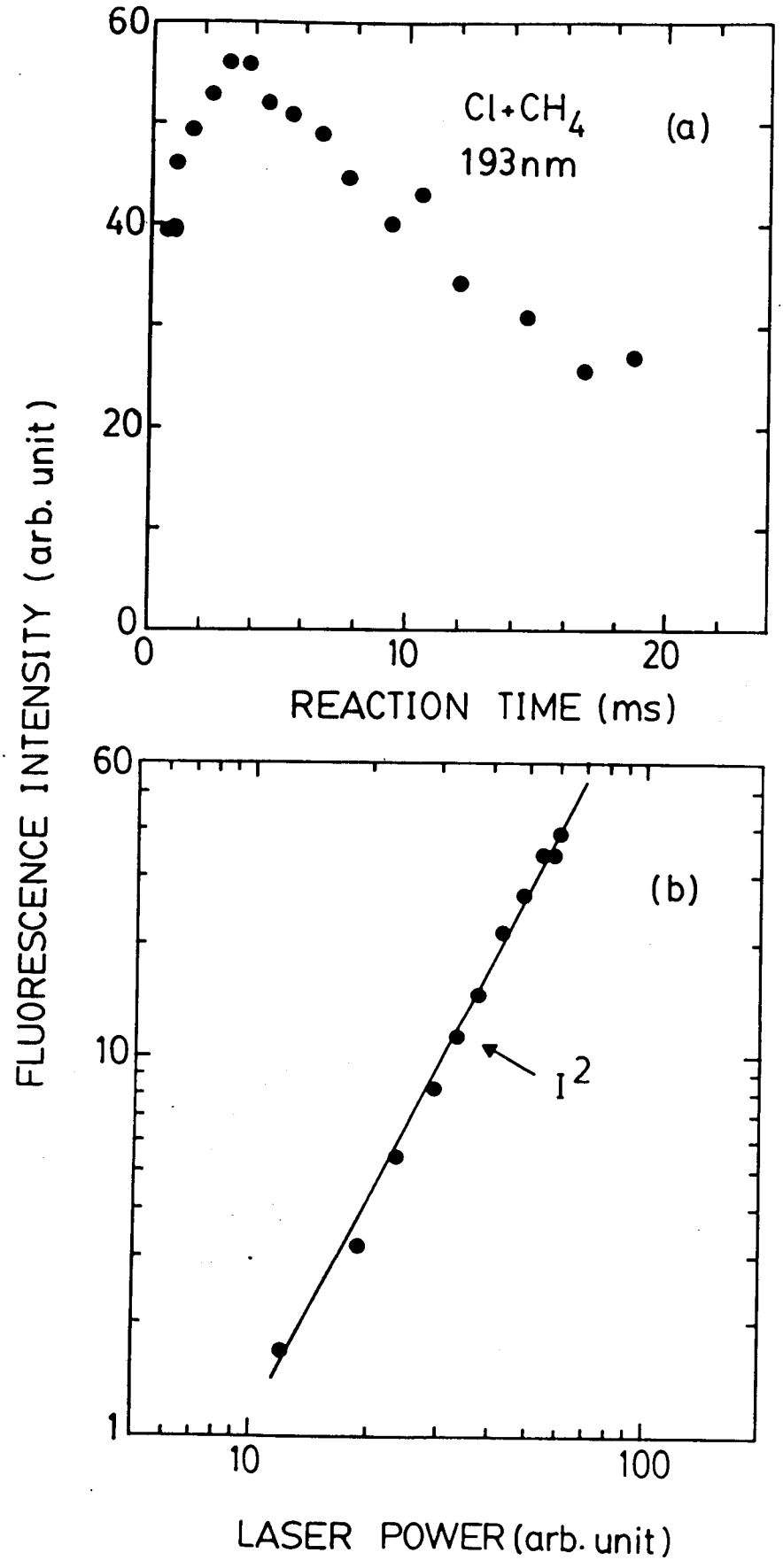
60
40
20
0
0
10
20
Cl+CH4
193nm
(a)
REACTION TIME (ms)
FLUORESCENCE INTENSITY (arb. unit)
60
10
1
10
100
(b)
I2
LASER POWER (arb. unit)

Fig 7

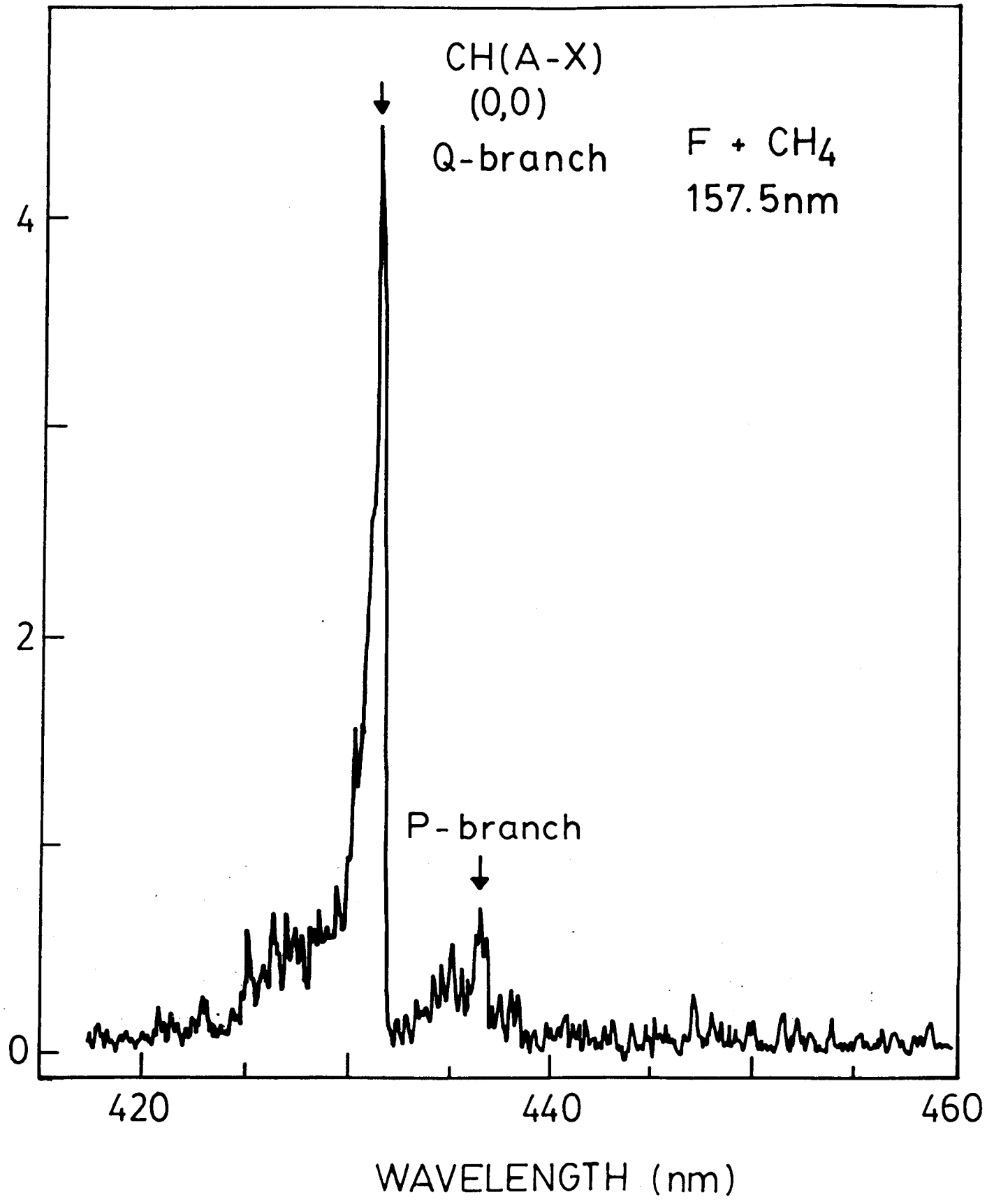
CH(A-X)
(0,0)
Q-branch
F + CH4
157.5nm
P-branch
4
2
0
420
440
460
WAVELENGTH (nm)

Fig. 8

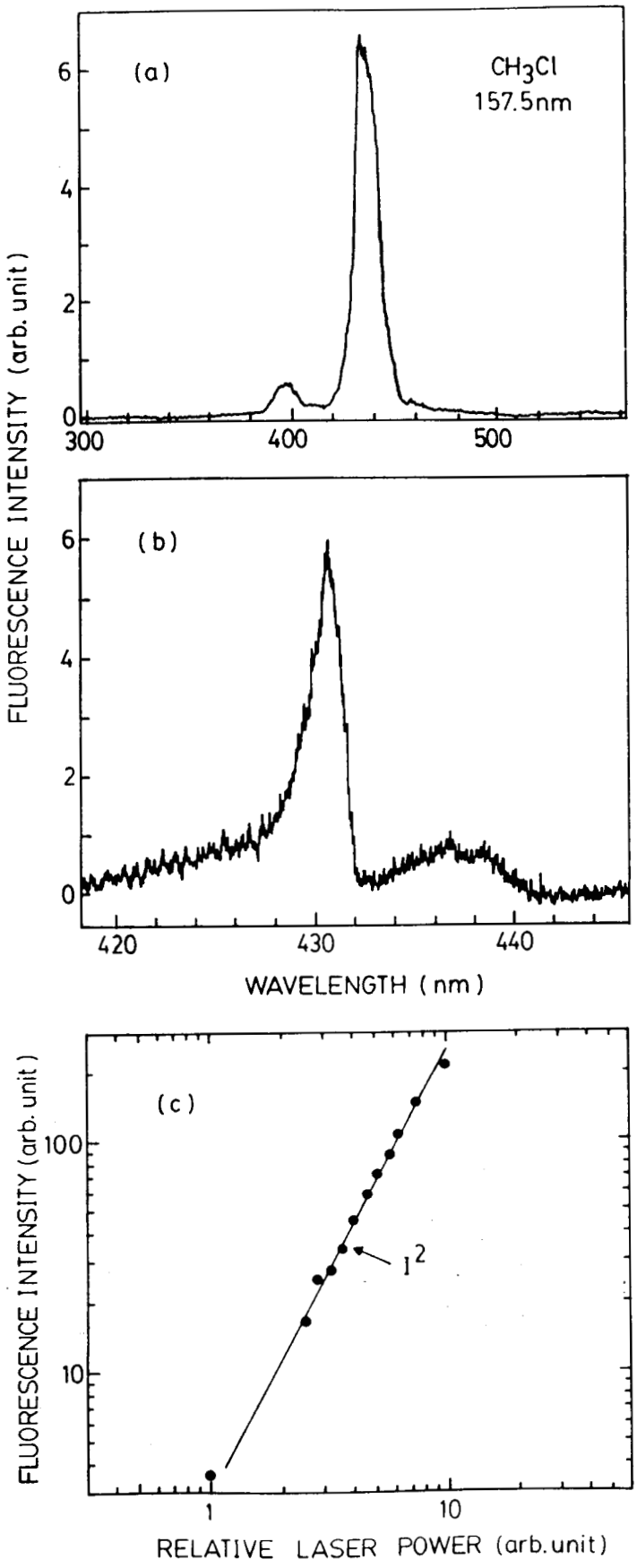
(a)
CH_3Cl
157.5nm
6
4
2
0
300
400
500
(b)
6
4
2
0
420
430
440
WAVELENGTH (nm)
FLUORESCENCE INTENSITY (arb. unit)
(c)
100
10
I^2
1
10
RELATIVE LASER POWER (arb.unit)
FLUORESCENCE INTENSITY (arb. unit)

Fig. 9

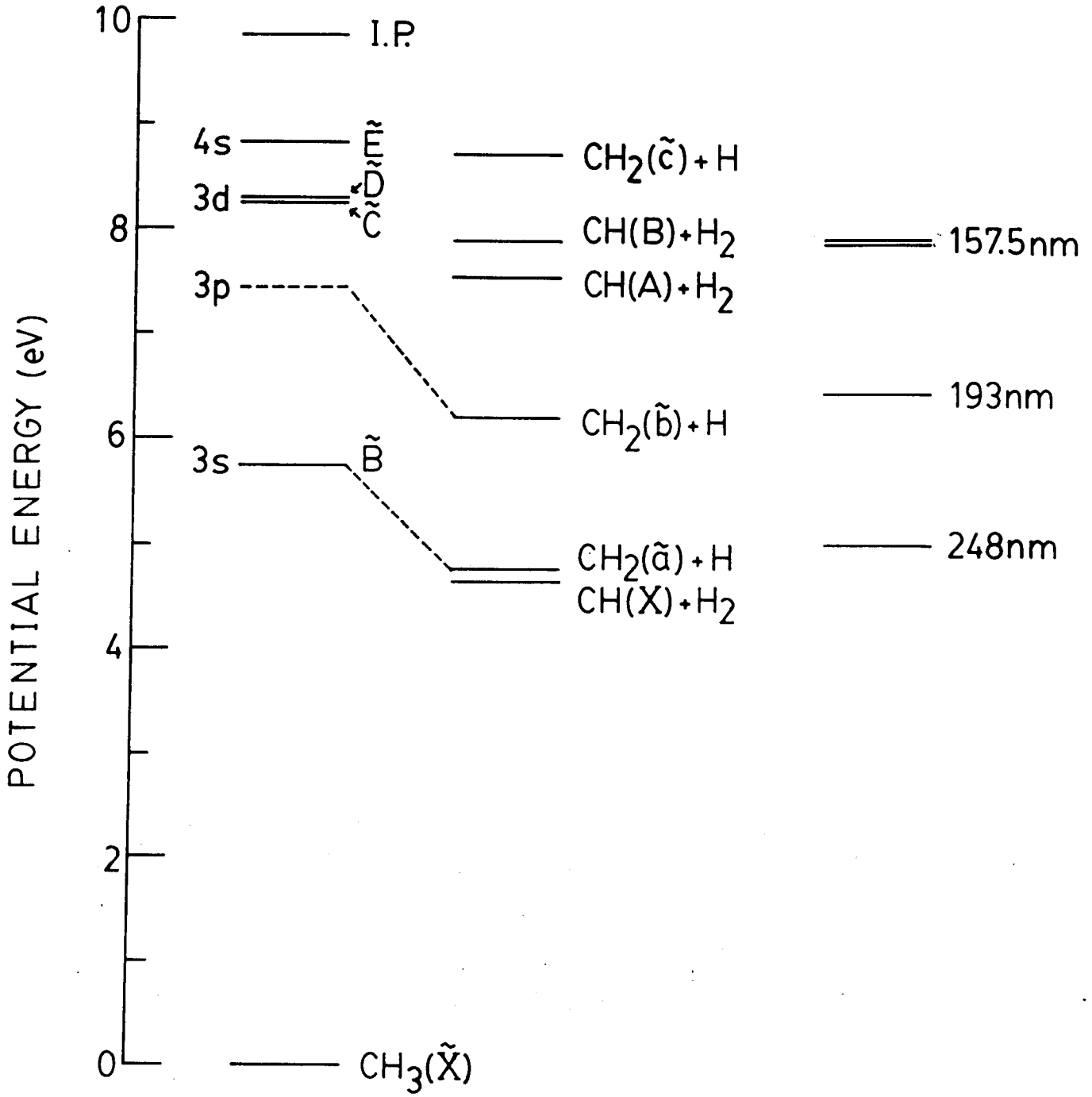
POTENTIAL ENERGY (eV)
10
8
6
4
2
0
I.P.
4s
3d
3p
3s
Ẽ
D̃
C̃
B̃
CH2(c̃) + H
CH(B) + H2
CH(A) + H2
CH2(b̃) + H
CH2(ã) + H
CH(X) + H2
CH3(X̃)
157.5nm
193nm
248nm

Fig. 10